Since January 2020 Elsevier has created a COVID-19 resource centre with free information in English and Mandarin on the novel coronavirus COVID-19. The COVID-19 resource centre is hosted on Elsevier Connect, the company's public news and information website.

Ceramics International 46 (2020) 15740–15763

Contents lists available at ScienceDirect

Ceramics International

journal homepage: www.elsevier.com/locate/ceramint

Review article

A review on MnZn ferrites: Synthesis, characterization and applications

Preeti Thakur[a], Deepika Chahar[a], Shilpa Taneja[a], Nikhil Bhalla[b,d], Atul Thakur[c,*]

[a] Department of Physics, Amity School of Applied Sciences, Amity University Haryana, Gurgaon, Haryana, 122413, India
[b] Nanotechnology and Integrated Bioengineering Centre (NIBEC), School of Engineering, Ulster University, Jordanstown, Shore Road, BT37 0QB, Northern Ireland, United Kingdom
[c] Centre for Nanotechnology, Amity University Haryana, Gurgaon, Haryana, 122413, India
[d] Healthcare Technology Hub, Ulster University, Jordanstown Shore Road, Northern Ireland, BT37 0QB, United Kingdom

ARTICLE INFO

Keywords:
Resistivity
Permeability
Permittivity
Coercivity
Transformers
Inductors
Transducers

ABSTRACT

Researchers are taking great interest in the synthesis and characterization of MnZn ferrites due to their wide range of applications in many areas. MnZn ferrites are a class of soft magnetic materials that have very good electrical, magnetic and optical properties. The properties of MnZn ferrites include high value of resistivity, permeability, permittivity, saturation magnetization, low power losses and coercivity. The above mentioned advantageous features of MnZn ferrites make them suitable for the use in various applications. In biomedical field these ferrites are used for cancer treatment and MRI. MnZn ferrites are also used in electronic applications for making transformers, transducers and inductors. These ferrites are also used in magnetic fluids, sensors and biosensors. MnZn ferrite is highly useful material for several electrical and electronic applications. It finds applications in almost every household appliances like mobile charger, LED bulb, TV, refrigerator, juicer mixer, washing machine, iron, microwave oven, mobile, laptop, desktop, printer and so on. Therefore, the present review focuses on different techniques for synthesis of MnZn ferrites in literature, their characterization tools, effect of doping on the properties of MnZn ferrite and finally we will discuss about their applications.

1. Introduction

A ferrite [1–6] is a ceramic material that is made up of iron oxide (Fe_2O_4) in large proportion mixed with metallic element such asbarium (Ba), manganese (Mn), nickel (Ni), zinc (Zn) in small proportions. The nature of both the iron oxide and the metal is electrically non-conducting and ferrimagnetic. Ferrimagnetic material is one that possesses unequal opposing magnetic moments which allow such materials to retain spontaneous magnetization. Ferrites are generally classified into two types: hard ferrites [7,8] and soft ferrites [9–17]. Hard ferrites have high coercivity and such materials are difficult to magnetize. Therefore these materials are used in making permanent magnets which are used for applications in refrigerator, loudspeaker, washing machine, TV, communication systems, switch mode power supplies, dc-dc converters, microwave absorbing systems, high frequency applications, refrigerator, loudspeaker etc. [18–25]. On the other hand, soft ferrites have low coercivity as a result of which their magnetization can easily be altered. Soft ferries are good conductors of magnetic field which has led to its wide range of applications in electronic industry such as developing transformer cores, high frequency inductors and as microwave components [26–42], see Fig. 1 for more details. Furthermore, advantages of soft ferrites include high resistivity, low cost, time and temperature stability, low loss and high permeability [43–46]. Most common soft ferrites are MnZn ferrites [47–55] and NiZn ferrites [56–73]. MnZn ferrites are more preferred as they have high permeability [74] and saturation magnetization [75]as compared to NiZn ferrites. Because of low value of resistivity of MnZn ferrites as compared to NiZn ferrites, these ferrites are used for low frequency applications [76–78]. The properties of MnZn ferrites are essentially dependent on the synthesis methods [55,79–85] and the doping concentrations inside nanoferrites [86,87].

In the past decade MnZn have attracted a large amount of attention in academia due to its advantageous features that make MnZn ferrites suitable to be used in many applications of daily life. The data of the publications of the MnZn ferrites by web of science in the last decade is shown in Fig. 2. The record of the data shows that there is a regular increase in the publications of the MnZn ferrite documents in the last ten years and much more progress in citations may be seen in years 2018 and 2019.

Fig. 3 shows various applications of MnZn ferrites. The change in the concentration of cations [88–92] and sintering conditions [93,94] changes the magnetic, electrical properties and structural properties of

* Corresponding author.
E-mail addresses: pthakur@ggn.amity.edu (P. Thakur), athakur1@ggn.amity.edu (A. Thakur).

https://doi.org/10.1016/j.ceramint.2020.03.287
Received 10 March 2020; Received in revised form 26 March 2020; Accepted 30 March 2020
Available online 07 April 2020

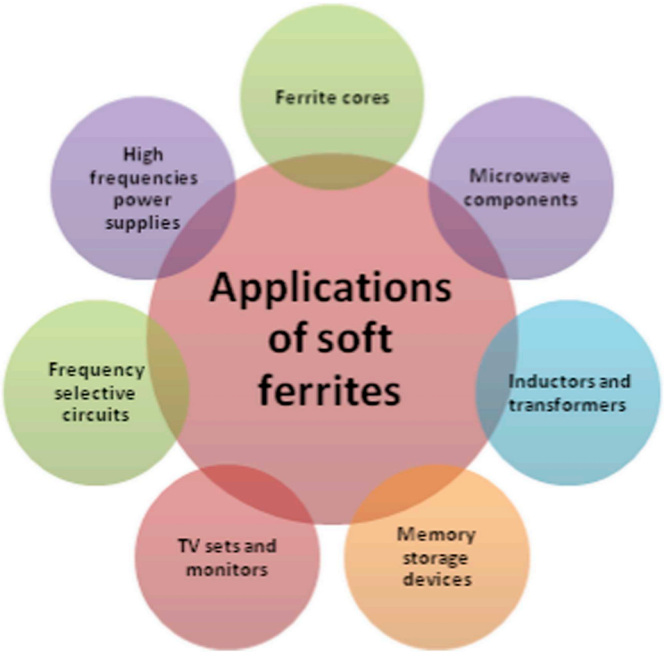

Fig. 1. Applications of soft ferrites

nanoferrites which lead to its wide range of applications. In addition, the shape, morphology, electrical, magnetic properties are affected by the cation distribution in the MnZn ferrite [95]. Cationic distribution for $Mn_{1-x}Zn_xFe_2O_4$ is described in Table 2. Considering the importance of Mn–Zn ferrites for various applications, a comprehensive review based on 261 references is summarized.

2. Purpose of the review

The main purpose of the review is to focus on the synthesis, morphology, properties and characterization methods of MnZn ferrites. While the subject of magnetic nanostructures is enormously wide and a large number of good review articles are published on magnetic nanoparticles, MnZn ferrites in particular constitute a special niche of nanoparticles because of immense interest of the scientific community in soft ferrites. In addition, this review critically analyze methods and discusses on the choice of synthesis method for use of MnZn ferrites in a given application. In brief methods such as sol-gel method [96–101], co-precipitation method [85,102–109], conventional ceramic technique [110,111], hydrothermal method [112–114], citrate precursor method [115–117], solid state reaction method [118], auto-combustion method [119] and microemulsion method [120] for the synthesis of MnZn ferrites are discussed. Various advantages and disadvantages of the synthesis methods are shown in Table 1.

3. Morphology of MnZn ferrites

MnZn ferrites have spinel structure [121]. The spinel structure has one major unit cell composed of 8 sub-unit cells having face centered cubic (FCC) structure with two types of sites in each unit cell i.e. tetrahedral (A) site and octahedral (B) site in the complete structure of MnZn ferrite. There are 64 tetrahedral interstitial sites and 32 octahedral interstitial sites. Spinel structure has closed packed oxygen atoms arrangement in which 32 oxygen atoms form a unit cell. Tetrahedral (A) sites are surrounded by four nearest neighbor oxygen atoms and octahedral (B) sites have six nearest oxygen atoms around it as shown in Fig. 4. In MnZn spinel ferrite lattice, Zn ions are on the tetrahedral sites while Fe and Mn ions occupy both tetrahedral and octahedral sites. Due to this spinel structure, different metallic ions can be introduced that causes change in the electric and magnetic properties of ferrites. The metal ions introduced may enter the spinel crystal lattice by replacing Fe^{3+} ions and leading to aggregation of these ions on the grain boundary. These morphological features suggest that the properties of MnZn ferrite nanoparticles can be tuned as long as the nanoparticle designer is specifically for a given application choose appropriate synthesis and characterization techniques. In order to know the best advantages of MnZn ferrites for various applications, one has to be aware of different synthesis and characterization techniques.

4. Why do we prefer MnZn ferrites?

MnZn ferrites are preferred over other ferrites due to their low cost and wide range of applications. These ferrites are very important for stress insensitivity and low noise and are generally used for applications where frequency requirements are below 2 MHz. MnZn ferrites are also advantageous due to their almost zero magnetocrystalline anisotropy.

In the class of soft ferrites, MnZn ferrites are preferred due to high permeability [122–127], saturation induction [128–130], low power losses [34,131–138] and high magnetic induction [139,140]. MnZn ferrites are of great interest due to their wide range of applications such as hyperthermia applications [141], power applications [109–111,142–144], magnetic fluid [145], high frequency power supply [142], memory storage devices, TV sets, biomedicines [146], magnetic resonance, catalysis etc. There is a continuous progress in the size and shape control of MnZn ferrites and also on the morphological and magnetic properties of MnZn ferrites by using different methods [147] of synthesis like sol-gel method [96–98], co-precipitation method [85,102–109,143], conventional ceramic technique [110,111], hydrothermal method [112–114,148–150], citrate precursor method [115], solid state reaction method [118], auto-combustion method [119,151], microemulsion method [120]. The effect of doping on the structural and magnetic properties of pure MnZn ferrites is also taken into account.

5. Synthesis methods to prepare MnZn ferrites

There are two approaches to synthesize nanoparticles: top–down and bottom–up. Both these approaches are shown in Fig. 5(a). In top–down, a bulk material is broken down to get nanosized particles. This method has many limitations like generally metal oxides are used, requirement of very high temperature for the reaction, products are inhomogeneous, presence of impurities, crystal defects, broad size distribution and imperfection in surface structure. In bottom–up approach, small atomic building blocks fit together to produce nanoparticles. This is most favorable method for nanoparticles synthesis as the products in this method are homogeneous, highly pure and have narrow size distribution.

Various synthesis techniques are used to prepare MnZn ferrite nanoparticles [152–160]such as sol-gel mthod [161–164], polyol process [165],co-precipitation method [104,166,167], hydrothermal method [113], citrate precursor method [122], solid state reaction method [118], auto-combustion method, ceramic processing method [139]. Some of the techniques to synthesize MnZn ferrites are shown in Fig. 6. By doping other elements or oxides [168–171] the structural, electrical and magnetic properties of MnZn ferrite can be enhanced. For instance, Zaspalis et al. [172]observed that there was 17% improvement in the total power loss per volume when doping was done of Nb_2O_5 in pure MnZn ferrite. After doping there was reduction in the losses related to magnetostriction and stress related hysteresis losses. Also, the eddy current losses related to electrical resistivity were also reduced. Xiang et al. [173] prepared MnZn ferrite particles with Ce^{3+} doping and observed that no impurity phase was detected in the XRD pattern. It confirmed that Ce ions entirely got dissolved in spinel structure. This also led to an increase in the saturation magnetization and decrease in the coercivity of MnZn ferrites, leading to an overall improvement in

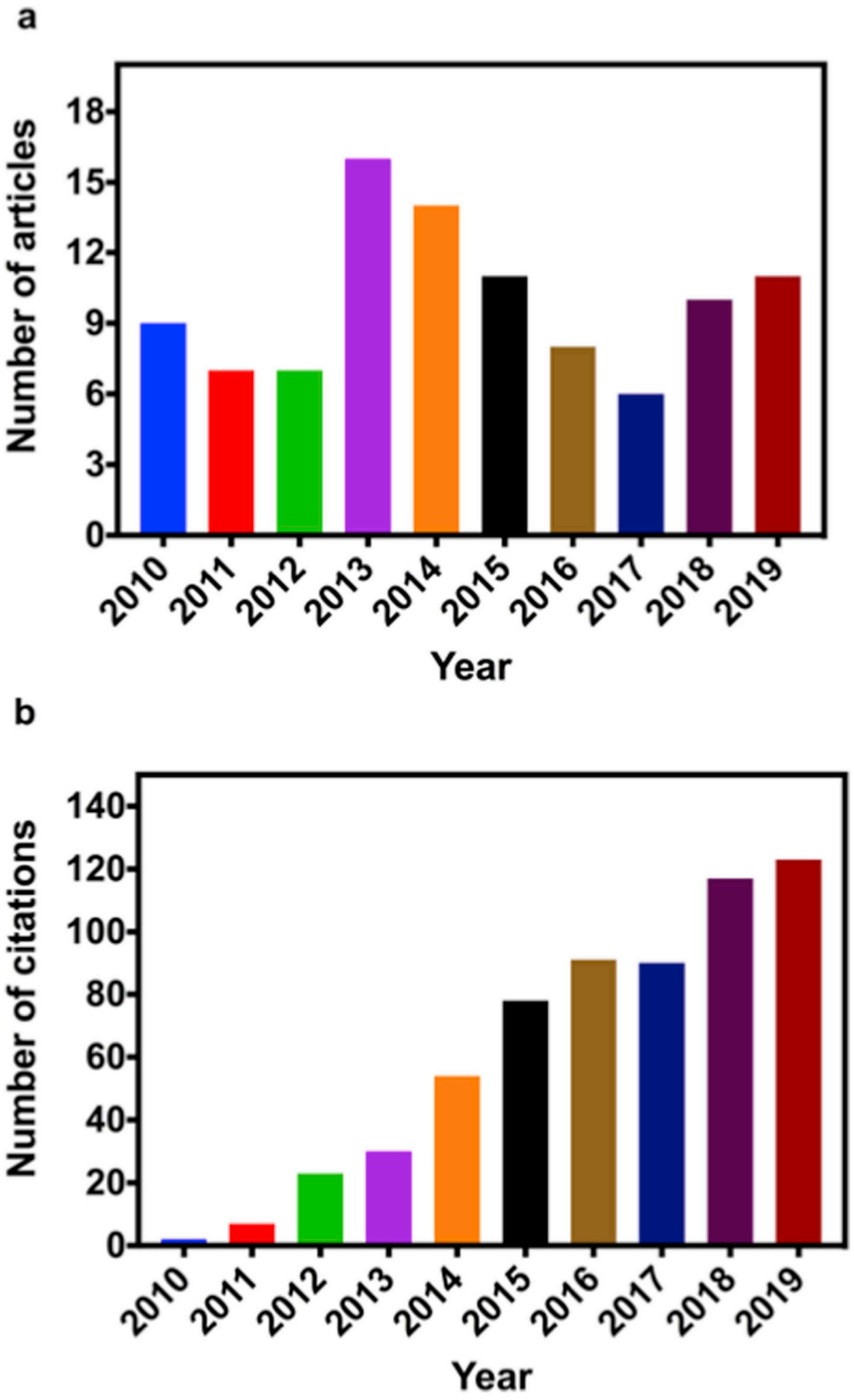

Fig. 2. Documents on MnZn ferrites in web of science in last 10 years a) number of articles and b) number of citations

the soft magnetic properties of the material. Some methods of synthesis are described below.

5.1. Microwave hydrothermal process

Microwave is a form of electromagnetic energy associated with electromagnetic field. It can be defined as an electromagnetic wave having frequency and wavelength between 300 MHz and 300 GHz in 1 m to 1 mm range respectively. While the study of microwaves started during 1930s, the first work on microwave hydrothermal synthesis of nanoparticles was demonstrated by Dr. Komarneni while distinguishing the traditional hydrothermal synthesis methods [174] from microwave hydrothermal synthesis [175–177]. In microwave hydrothermal method, heat required in the synthesis process is generated by microwaves which have the advantage of high penetrating power. Microwaves can penetrate and heat the sample to a certain depth. Microwave hydrothermal method is beneficial as it has very fast heating rates to allow generation of uniform nanomaterials with fine particle size

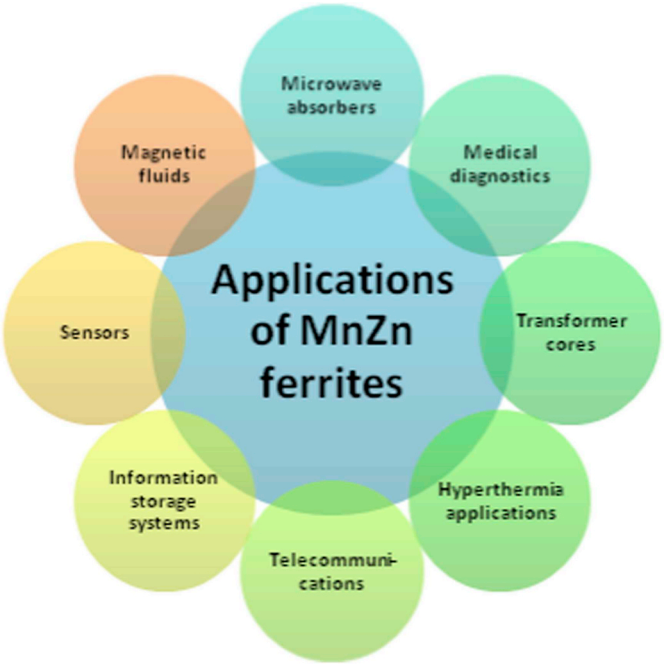

Fig. 3. Applications of MnZn ferrites.

distribution. Hence, this is faster, cleaner and economical method as compared to traditional hydrothermal method [178]. Praveena et al. [179] synthesized MnZn ferrites by using microwave hydrothermal process. Pure manganese nitrate [$Mn(NO_3)_2.6H_2O$], zinc nitrate [$Zn(NO_3)_2.6H_2O$] and ferric nitrate [$Fe(NO_3)_2.9H_2O$] were dissolved in 50 ml de-ionized water. In this process pH was maintained at about 9.4.Thereafter the mixture was sealed in tetrafluorometoxil (TFM) and was put in microwave oven for 30 min at 160°C followed by washing of the solids with de-ionized water and ethanol several times. The resulting wet mixture was dried and then polyvinyl alcohol (PVA) was added that acted as a binder. The powder was then pressed into pellets followed by sintering at 900°C for 30 min. Single phase spinel structure was confirmed by the XRD spectra.

Table 2
Cation distribution of $Mn_{1-x}Zn_xFe_2O_4$.

X	Cation distribution
0.2	$(Zn_{0.2}Mn_{0.4}Fe_{0.4})[Mn_{0.4}Fe_{1.6}]O_4$
0.4	$(Zn_{0.4}Mn_{0.2}Fe_{0.4})[Mn_{0.4}Fe_{1.6}]O_4$
0.6	$(Zn_{0.4}Mn_{0.2}Fe_{0.4})[Zn_{0.2}Mn_{0.2}Fe_{1.6}]O_4$
0.8	$(Zn_{0.6}Fe_{0.4})[Zn_{0.2}Mn_{0.2}Fe_{1.6}]O_4$

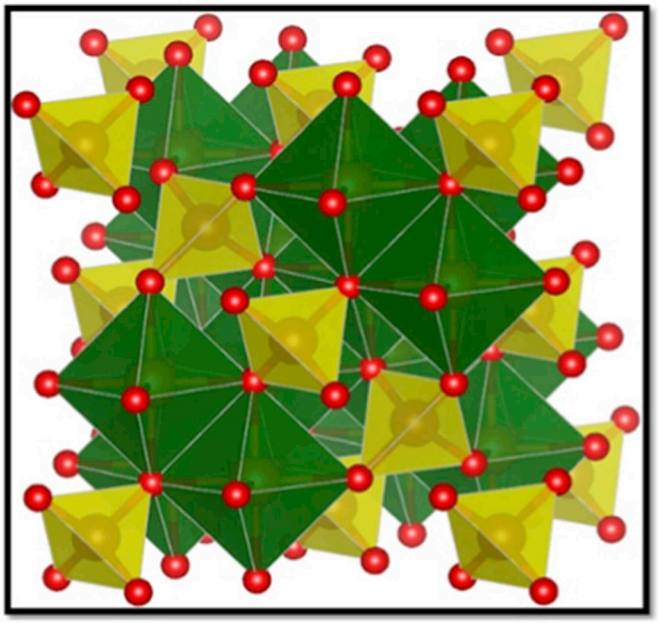

Fig. 4. Spinel structure(Reproduced by permission from Ref. [241],License Number: 4646900916646, Copyright 2016, Elsevier).

5.2. Hydrothermal method

The hydrothermal method is used for the preparation of ferrite nanoparticles on a large scale. Essentially, in this method the yield of nanoparticles is very high. If the parameters such as temperature, pressure and reaction time are properly selected, good quality

Table 1
Summary of advantages and disadvantages of major synthesis techniques.

Methods	Temperature (°C)	Advantages	Limitations
Co-precipitation	30–140	Simple process Aqueous media Controlled size and morphology Easily functionalized	Poor crystallinity Very long reaction time required Broad size distribution
Hydrothermal	100–200	Scalable Controlled size Aqueous media High yield	Requirement of special reactor High pressure required (> 2000PSI) High temperature Long reaction time
Sol-gel method	20–200	Controlled size and shape Low cost	Takes longer time Yield is medium
Microwave hydrothermal method	160	Fast heating speed Faster and economical Very fine nanoparticles produced Uniform morphology	–
Combustion method	480	Less time and energy required Simple and effective method Versatile and fast Nanoparticles produced are pure and homogeneous	Very high temperature is required
Solid state reaction method	25	No toxic and expensive solvent used Facile and economic	–
Oxidation process	30	Narrow size distribution Uniform size	Irregular and elongated morphology of the product

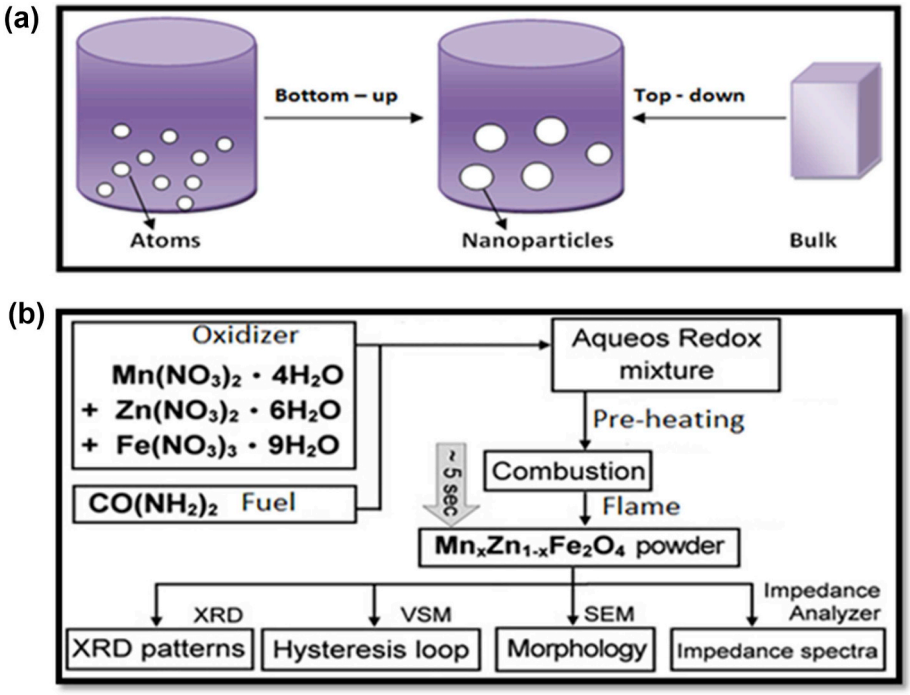

Fig. 5. (a) Top–down and Bottom–up approach to synthesize nanoparticles and (b) flow chart for preparation of MnZn ferrite by novel combustion method using subsequent heat treatments (Reproduced by permission from Ref. no. [259], Licence No. 4763520487833, Copyright 2011, Elsevier).

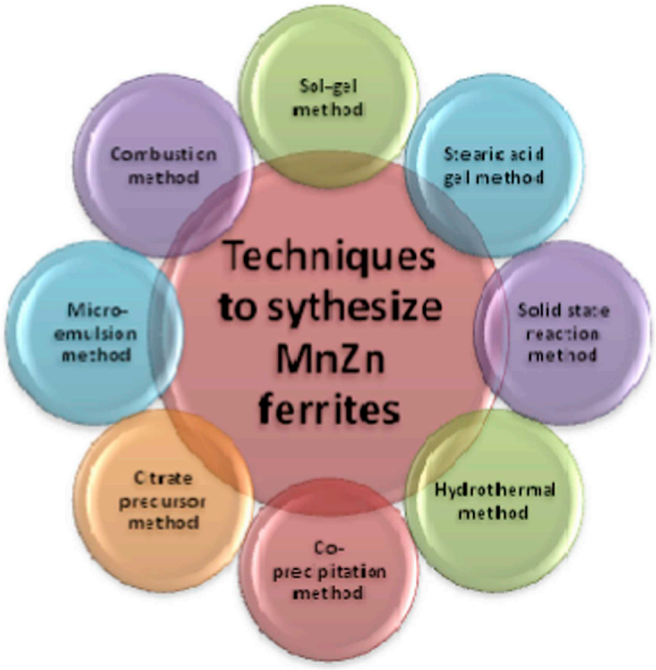

Fig. 6. Various synthesis techniques to synthesize MnZn ferrites.

nanoparticles can be synthesized. Phong et al. [112] studied magnetic properties and specific absorption of $Mn_{0.3}Zn_{0.7}Fe_2O_4$ nanoparticles. In this work the MnZn ferrites were prepared by a hydrothermal process in a Teflon-lined stainless steel autoclave. The starting materials $FeCl_3$, $MnCl_2$, $ZnCl_2$ were dissolved in HCl solution and NaOH was slowly added to the solution and stirred for 30 min. The solution was transferred to Teflon-lined stainless steel autoclave till it was 80% full. The autoclave was heated at 180°C for 12h and then left for cooling to room temperature. After that the products were washed many times with hot de-ionized water and acetone and finally dried in an oven at 80°C for 5h. By this method, large quantity of ferrite nanoparticles can be synthesized. The Mn-Zn ferrite nanomaterials prepared by this method have controlled size and this method requires aqueous media for the synthesis. But this method has some limitations that include requirement of special reactor, need of high pressure and high temperature.

5.3. Co-precipitation method

Co-precipitation [180] is an easy and conventional method to synthesize nanomaterials. The ferrites prepared using this method are of controlled size, highly pure and have homogeneous structure. Typical co-precipitation method for synthesis of nanoparticles is shown in Fig. 7. Normally inorganic salts (nitrate, chloride, sulphate, etc.) are used in this method as the starting materials that are dissolved in water or any other medium which is suitable to form a homogeneous solution. The pH of the solution is adjusted to 7–9 and the solvent is evaporated to get nanoparticle precipitates. It should be noted that the concentration of salt, temperature, pH and the rate of pH change are detrimental to crystal growth and aggregation of the particles. After precipitation, the solid mass is collected and washed. This is followed by heating of the residue up to the boiling point of the medium to dry the resultant product and form hydroxides. The hydroxides are then calcined to transform the hydroxide into crystalline oxides. Thakur et al. [181] used co–precipitation method to synthesize MnZn ferrite. In this method, manganese chloride, zinc chloride, iron(III) chloride and sodium hydroxide were used as raw materials. A 3 M solution was prepared in 60 ml of distilled water. This solution was then poured into boiling NaOH solution while stirring for 60 min at temperature 353–358K with a magnetic stirrer, maintaining the pH between 11 and 12. Stirring allowed precipitates of the nanoparticles to settled down and then sample was washed many times with distilled water. After washing, the sample was dried in hot air oven followed by crushing the resultant into powder using mortar pestle. Anwar et al. [9] also synthesized MnZn ferrites by the chemical co–precipitation method by taking solution of $Mn(NO_3)_2.4H_2O$, $Zn(NO_3)_2H_2O$ and $Fe_2(NO_3)_3.9H_2O$ as the starting materials. These were mixed to form homogeneous

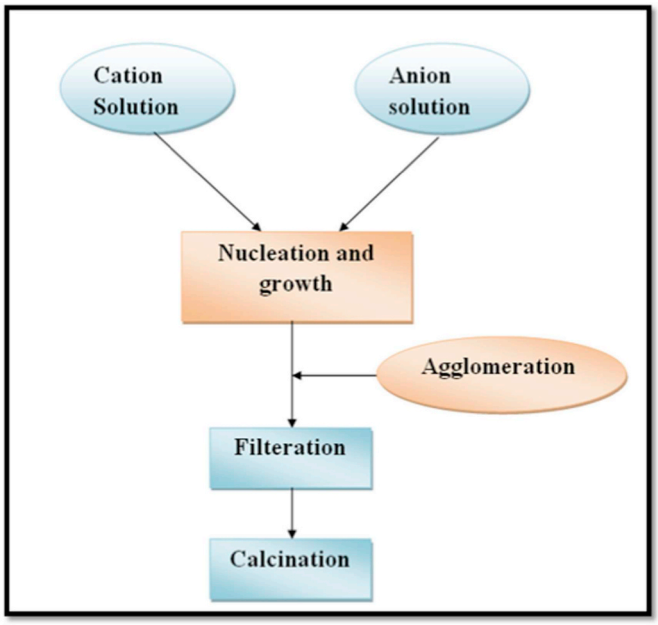

Fig. 7. Typical Co–precipitation method for Mn-Zn ferrite nanoparticles synthesis.

solution at 358K. Then, ammonia solution was added dropwise with constant stirring maintaining the pH between 10 and 11. The mixture was heated at 353K for 1h. Then after the washing and drying process the ferrite powder was heated at 673 K, 773K and 923K separately and pressed in the form of circular pellets. The chemical reaction during the process was:

$$0.5Mn(NO_3)_2.4H_2O + 0.5ZnNO_3.H_2O + 2Fe_2(NO_3)_3.9H_2O + 8NaOH \rightarrow 0.5Mn(OH)_2.0.5Zn(OH)_2.2Fe(OH)_3 + 2NaCl + 6NaNO_3 \rightarrow Mn_{0.5}Zn_{0.5}Fe_2O_4.nH_2O + (4\text{-}n)H_2O$$

Yadav et al. [182] studied the properties of ferrite nanoparticles by co–precipitation method with samarium doping. The ferrites with Sm doping were very pure and had single crystalline spinel phase. Kumar et al. [183] studied the conduction phenomena in indium substituted Mn–Zn nano-ferrites. $Mn_{0.4}Zn_{0.6}In_yFe_{2-y}O_4$ (y = 0. 0.035, 0.070, 0.100) were synthesized by oxalate co-precipitation method followed by microwave heating. The raw materials used were manganese sulphate monohydrate ($MnSO_4.H_2O$), iron sulphate heptahydrate ($FeSO_4.7H_2O$), zinc sulphate heptahydrate ($ZnSO_4.7H_2O$), anhydrous indium sulphate ($In_2(SO_4)_3$) and Diammoniumoxalate monohydrate [$(NH_4)_2C_2O_4.H_2O$]. These all starting materials were mixed by rapidly adding Di-ammonium oxalate under continuous stirring at 45 °C for 30 min until precipitates were formed. Precipitates were washed many times and then dried in an oven at 100 °C for 8h. Dried yellow precipitates were used to prepare ferrites by using in-house built microwave heating set up. Aluminium metal powder was used as microwave susceptor. This set up was then put on a commercial microwave oven operated at a frequency 2.45 GHz. The oven was set to raise the temperature to 450 °C. Then, brick was taken out and allowed to cool. Co–precipitation method has several advantages as it uses aqueous medium for synthesis and also the synthesis is very simple. There is a good control on the size and morphology of the nano particles formed. But this method takes long time to synthesize nanoferrites. This method is disadvantageous due to poor crystalline nature of the resultant ferrite powder.

5.4. Sol–gel method

Sol–gel method [184,185] is a promising method used for the preparation of ferrite nano materials. It is a chemical solution process used

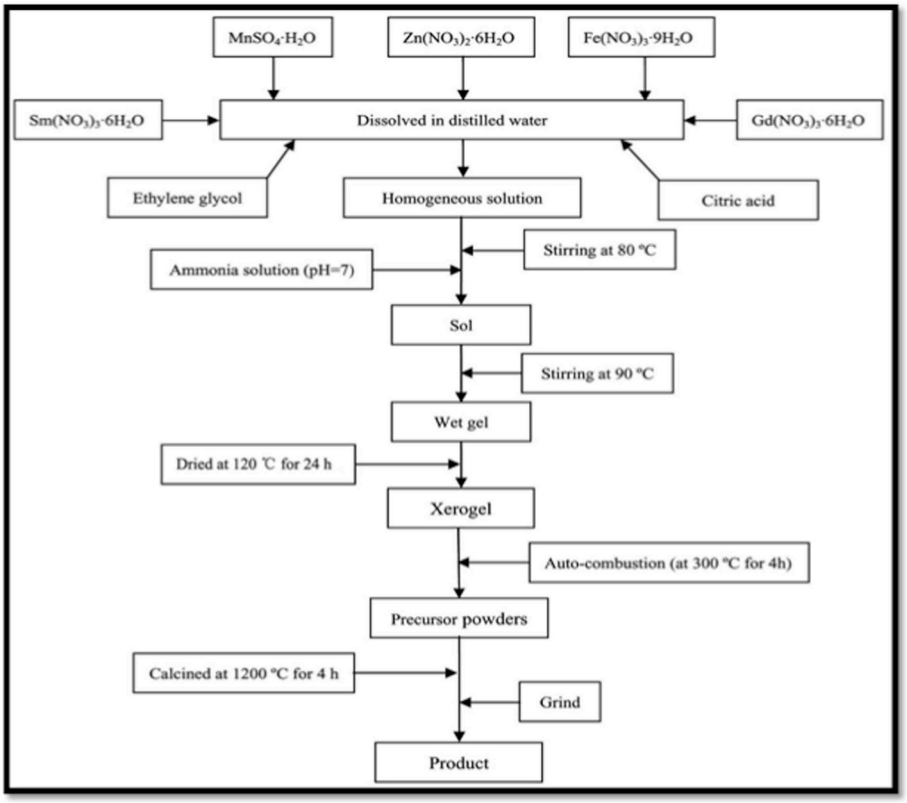

Fig. 8. Flow chart for the preparation of samples using sol-gel auto combustion method (Reproduced by permission from Ref. [240], Licence No. 4763510638098, Copyright 2016, Elsevier).

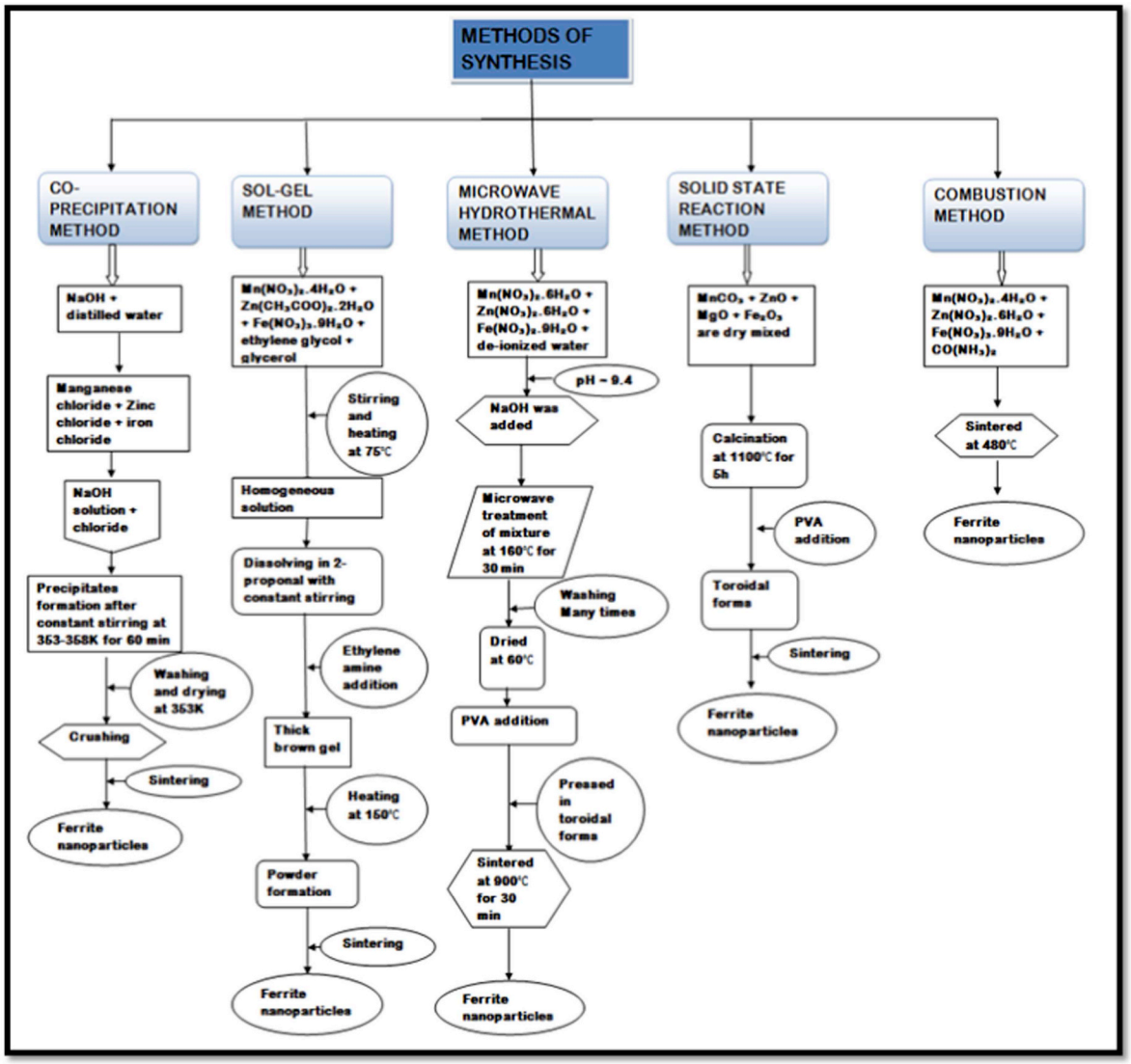

Fig. 9. Different methods of synthesis for preparation of MnZn ferrite.

to synthesize nanoparticles. A sol is a colloidal or molecular suspension of solid particles of ions in a solvent and gel is a semi–rigid mass that forms when the solvent from the sol starts evaporating where the particles left behind start to join together in a continuous network. The resultant product which comes out is in the form of colloidal powder or films. This method is advantageous because of controlled microstructure of the final product. The resultant particles formed are of uniform and small size. Also, this technique of nanoparticles synthesis is economical and it involves use of low temperature. Duan et al. [161] synthesized MnZn ferrite nanoparticles taking pure $Fe(NO_3)_3.9H_2O$, $Zn(NO_3)_2.8H_2O$ and $Mn(NO_3)_2$as starting materials. These materials were dissolved in de-ionized water at 60°C. Also, $C_6H_8O_7.H_2O$ was dissolved in above solution to chelate the metal ions with the citrate ions and concentration was adjusted to 0.1–0.4 by adding de-ionized water. PVP was added as a binder to reduce film cracks. The spin coating was done at 3000 rpm for 30s. The samples were heated at 350°C for 30min, followed by crystallization at 550°C for 60min after each coating. The flow chart of the sol-gel auto combustion method is shown in Fig. 8. The sol-gel method is also used for depositing structurally and magnetically uniform films for spin thermoelectric generator. Gabal et al. [186] studied Mn–Zn nano-crystalline ferrites synthesized from spent Zn–C batteries using novel gelatin method. The Zn–C batteries were used to synthesize the ferrites by using sol-gel method using gelatin. Jalaiah et al. [187] synthesized nickel doped MnZn ferrites by sol–gel auto combustion method and observed non-collinear magnetic structure. The room temperature conductivity was observed to be higher than pure MnZn ferrite. There was a decrease in dielectric constant and dielectric loss tangent with increase in nickel concentration.This method is advantageous because of better size and shape control but it takes a longer time to complete the synthesis. Sol-gel method is a simple process, require low processing temperature and low cost. The prepared ferrite consists of a pure cubic spinel structure.

5.5. Combustion method

Combustion process is the effective and low cost method to synthesize nano materials. This process is simple, versatile and fast for nano material preparation. This method is advantageous as less time and energy is spent during the synthesis process. The nanoparticles produced are pure and homogeneous. Many researchers synthesized MnZn ferrites by using this method [188,189]. Manganese nitrate [$Mn(NO_3)_2.6H_2O$], zinc nitrate [$Zn(NO_3)_2.6H_2O$], iron nitrate [$Fe(NO_3)_3.9H_2O$] were taken in proper proportions and urea [$CO(NH_2)_2$] was used as a reducing agent in this process. Typically a solution is formedby adding these all materials in de–ionized water and heated on a hot plate at 480°C in air. Then, it is ignited within 5 s with flame

temperature ~1600°C. Combustion technique methodology is described in Fig. 5. While doping with other elements, a decrease in the lattice parameter was observed which could be attributed to the fact that ions of doped elements get trapped at the grain boundaries. Hence they hinder the grain growth and may cause an increase in strain on the grains that leads to decrease in lattice parameter. Doping of rare–earth metals can be done using combustion method [189] in a single step. The fuel chosen in the combustion methodalso has very important effect on the MnZn ferrites prepared. The fuels that are generally preferred in this method are urea and glycine. By using these fuels uniform nanoferrites with controlled stoichiometry are obtained.

5.6. Solid state reaction method

The solid-state reaction method to synthesize nanoparticles has several advantages. In this method, toxic and expensive organic solvents are not used in the reaction and all the materials used to synthesize MnZn ferrite nanoparticles are easily available and cost effective. The synthesis process is performed at room temperature under atmospheric pressure which is facile and economic. Many researchers synthesized MnZn ferrites by using this method [30,132,134,190]. The raw materials $MnCO_3$, ZnO and Fe_2O_3 in the proper weight were powdered and the powdered samples were calcined at 1100°C for 5h in air atmosphere using muffle furnace with heating rate of 10°C/min and a cooling rate of 5°C/min. Then, PVA was used as a binder and powder was pettelized into small disks and torroids. Then sintering was done to get the required nano ferrites. Kogias et al. [191] studied MnZn ferrite with low losses at 500 kHz over a broad temperature range by preparing MnZn ferrite using conventional ceramic technique of solid state reaction.Tsakaloudi et al. [192] studied process and material parameters towards the design of fast firing cycles for high permeability MnZn ferrites. In this paper, high permeability of MnZn ferrites was reduced by increasingthe energy consumption in the synthesis reaction due to prolonged sintering process for the production of nanoferrites. Zapata et al. [30] studied effect of zinc concentration on the microstructure and relaxation frequency of Mn–Zn ferrites synthesized by solid state reaction. Rahaman et al. [193] studied synthesis, structural, and electromagnetic properties of Mg doped ferrites. Fig. 9 shows the flow chart of various synthesis techniques.

5.7. Oxidation method

Oxidation method is a chemical method to prepare ferrite nanoparticles. The ferrite particles synthesized are irregular, have elongated morphology. The advantage of this method is that the particles have narrow size distribution and uniform size but by using this method ferrite colloids of small size are formed. Joseyphus et al. [41] prepared MnZn ferrite by using oxidation method. The synthesis procedure of nanoparticles by oxidation method is shown in Fig. 10. Proper amounts of $FeSO_4.7H_2O$, $MnCl_2.4H_2O$, $ZnSO_4.H_2O$ and $Fe_2(SO_4)_3$ were used as starting materials to synthesize $Mn_{0.67}Zn_{0.33}Fe_2O_4$. The weighed amounts of $FeSO_4.7H_2O$, $MnCl_2.4H_2O$, $ZnSO_4.H_2O$ and $Fe_2(SO_4)_3$ were dissolved in 250 mL water and then the mixture was allowed to react with NaOH dissolved in 250 mL of water. Constant stirring was done for 2h to oxidize the metal hydroxide precipitates by adding KNO_3. The pH was maintained between 12 and 13. Washing of the precipitates was done many times and then these were allowed to dry in an oven at 333K for 2 days.

5.8. Nitrilotriacetate precursor method

By using this method we can synthesize MnZn ferrite at a very lower temperature. Tangsali et al. [194] synthesized $Mn_xZn_{1-x}Fe_2O_4$ (x = 0.3, 0.35, 0.4, 0.45, 0.5, 0.55, 0.6, 0.65, 0.7) by using this method. All the metal salts were mixed in proper amounts in aqueous solution of dihydrazinium nitrilotriacetate. Dry precursors of nitrilotriacetate hydrazinate of metal ions were obtained from the solution and ignited. Then the autocombustion of the dry precursors resulted in the formation of metal oxides. Tangsali et al. [195] also studied the effect of sintering conditions on the resistivity of MnZn ferrite nanoparticles prepared by using this method. The resultant products in this technique showed high saturation magnetization and high values of Curie temperature that was between 750K and 380K.

5.9. Stearic acid gel method

Stearic acid or octadecanoic acid ($CH_3(CH_2)_{16}COOH$) is a common fatty acid that exists as glycerol ester in animal and plant fat. Many researchers used stearic acid gel to synthesize nanomaterials. Jafarnejad et al. [196] used this method to synthesize $MgCr_2O_4$ and Enhessari et al. [197] synthesized $CoTiO_3$ by using stearic acid gel method. Ma et al. [198] synthesized MnZn ferrite with chemical formula $Mn_xZn_{1-x}Fe_2O_4$ by using stearic acid gel method. Proper amounts of $MnCO_3$, $Zn(NO_3)_2.6H_2O$ and $Fe(NO_3)_2.9H_2O$ were powdered and mixed with Stearic acid in molten form. Stirring was done for 3–4h after heating the mixture in oil bath at 120°C. This resulted in formation of a brown gel. The gel was cooled in air and then powdered by grinding it. This was followed by washing of the grinded mixture with water three times followed by drying of this mixture at 100°C. MnZn ferrites were obtained by heating at 450°C for 1 h.

6. Characterization

The characterizations of MnZn ferrites are done with various instruments such that X-ray diffractometer, scanning electron microscopy [199–201], transmission electron microscopy and atomic force microscope (AFM). The magnetic properties of the ferrites are studied by vibrating sample magnetometer (VSM), magnetization hysteresis (M − H) loops [202] and electron spin resonance (ESR) hysteresis loop measurements. The X-ray investigation is done using X-ray diffractometer with CuKα radiation (λ = 1.5405 Å). Various formulas for the determination of lattice constant, X-ray density and crystallite size are listed below.

Measurement of lattice constant (a): From the analysis of XRD data, the lattice constant can be calculated using the formula:

$$a = d_{hkl}(h^2 + k^2 + l^2)^{1/2} \quad (1)$$

where a is the lattice constant, d is the interplanar spacing, and h, k, and l are the miller indices.

Measurement of X-ray density ($d_{x\text{-}ray}$): Theoretical density can be calculated using the relation:

$$d_{xrd} = 8M/Na^3 \quad (2)$$

where M is the molecular mass of each component, N is the Avogadro's number (6.023×10^{23} particles/mol).

Measurement of Experimental density (d_{exp}): Experimental density can be measured using the formula:

$$d_{\exp} = mass/volume \quad (3)$$

Measurement of crystallite size (D): Crystallite size is calculated by using the Scherrer's formula:

$$D = \frac{0.9\lambda}{\beta \cos\theta} \quad (4)$$

where D is the crystallite size, λ = 1.54056 Å is the wavelength of X-ray, θ is Bragg's angle and β is the FWHM value.

6.1. Size and shape

Many techniques are used to determine the shape, size and morphology of magnetic nanoparticles such as XRD, SEM, TEM, HRTEM

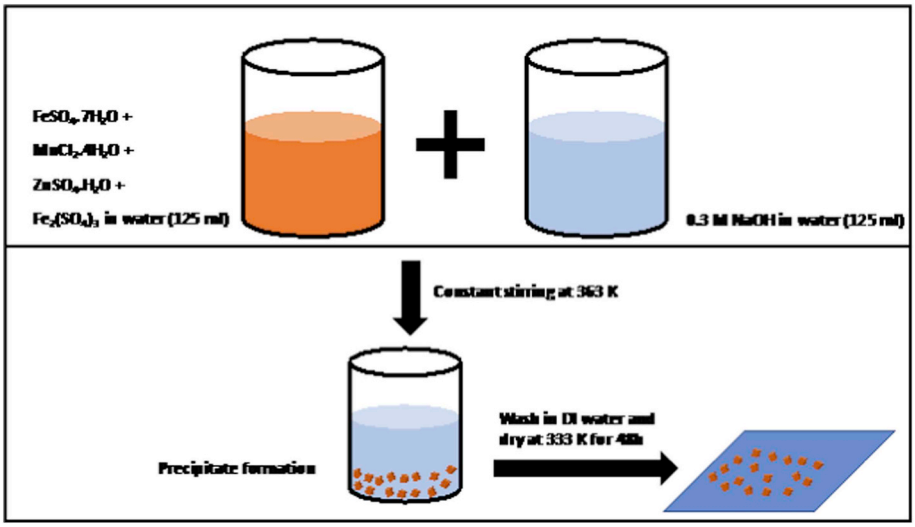

Fig. 10. Synthesis techniques of oxidation method.

(High resolution transmission electron microscopy) and FESEM (Field-emission scanning electron microscopy). By using HRTEM we can get information about shape, size, crystallinity and lattice spacing. XRD is used to determine the size by using Scherrer equation. However, SEM is better than XRD as XRD cannot determine the size of very small magnetic nanoparticles.

6.1.1. XRD analysis

Ramiza et al. [102] studied the effect of UV radiations to control particle size of Mn–Zn spinel ferrite nano-particles. From the XRD analysis it was observed that with the UV radiations minimum particle size was obtained i.e. 6.198 nm. The size of the sample that was not UV treated was found to reduce from 90 nm to 50nm and the crystallite size of the pure MnZn ferrites was found to be in the range 25 nm–35 nm in almost all cases as described in Table 3. The lattice parameter was found to be in the range 8.30Å–8.570 Å. Praveena et al. [179] observed that the lattice constant lie between 8.302 Å and 8.311 Å according to composition. The bulk density and the X-ray density increased from 4.98 gm/cm^3 to 4.90 gm/cm^3 and 5.12 gm/cm^3 to 4.98 gm/cm^3. Thakur et al. [203] studied effect of sintering temperature and observed that the average crystallite size was found to increase with an increase in sintering temperature i.e. from 11.38 nm to 67.42 nm. Also, the lattice constant was found to increase from 8.409 Å to 8.483 Å with increasing sintering temperature. At 1373K, a well crystallized single MnZn ferrite phase was formed. Mirshekari et al. [204] observed from the XRD that the average crystallite size was in the range 43.25 nm–66.7 nm. Small amount of lattice strains were also observed improving its magnetic properties. Anwar et al. [9]studied the effect of sintering temperature and observed that the pure MnZn ferrite had pure spinel structure and at 673K sample had cubic spinel structure. At 923 K, the XRD pattern contained additional reflections which were due to Fe_3O_4. The crystallite size increased from 7 to 13 nm. The lattice constant decreased from 8.439 Å to 8.431 Å with an increase in sintering temperature from 673K to 923K. The XRD density was found in between 5.21g/cm^{3}and 5.23 g/cm^3 as described in Table 3. Gabal et al. [186] observed from the XRD analysis that MnZn ferrites had a single phase cubic spinel structure with characteristic (311) reflection on 2Θ = 34.58 and no diffraction peak due to impurity was observed. The broad diffraction peaks were observed showing ultrafine nature and small crystallite size. The lattice parameter showed a decreasing value from 8.4466 Å to 8.4164 Å with increasing Zn content and the density increased from 5.13 g/cm^3 to 5.32 g/cm^3. Phong et al. [112] observed that the XRD pattern showed single phase spinel cubic structure with Fd3m space group. The lattice parameter was calculated 8.432 Å and x-ray density was 5.27 g/cm^3. The average crystallite size was 14 nm. Further from the XRD patterns [30], it was observed that the cubic spinel phase was formed and slight contraction was observed in lattice parameter from 8.4749 Å to 8.4353 Å as Zn concentration increased because Zn^{2+} ions (0.082 nm ionic radii) replaced Mn^{2+} ions (ionic radii = 0.091 nm). The value of sintered density increased from 4.93 g/cm^3 to 4.96 g/cm^3 with increase in Zn content. Jalaiah et al. [187] observed that the lattice parameter found to vary from 8.4555 Å to 8.5758 Å. The average crystallite size was calculated by the Scherrer's formula and was found to be in the range 10 nm. In the XRD pattern as studied by Angadi et al. [189] observed the Braggs reflections that indicate the crystalline nature of the samples with cubic spinel structure corresponding to Fd3m space group. When Sc^{3+} concentration was increased, the peak shifted towards the lower 2θ angle because of the relative difference between the ionic radii of Sc^{3+} (0.745 Å) with that of Fe^{3+} (0.55 Å). A decrease in the lattice parameterwas observed from 8.434 Å to 8.431 Å on Sc^{3+} doping which could be due to presence of Sc^{3+} ions at the grain boundaries. In the XRD patterns, peaks showed the cubic spinel structure [190]. The lattice parameter of pure MnZn ferrite increased with increase in sintering temperature from 8.3383 Å to 8.3496 Å and decreased in Mg doped MnZn ferrite from 8.3542 Å to 8.3225 Å with increasing sintering temperature. Bulk density decreased with an increase in sintering temperature from 4.87 g/cm^3 to 4.45 g/cm^3 in pure MnZn ferrite and from 4.61 g/cm^3 to 4.57g/cm^{3}in Mg doped MnZn ferrite due to discontinuous grain growth. Islam et al. [128] studied structural, magnetic and electrical properties of Gd-substituted Mn–Zn mixed ferrites. From the XRD patterns it was concluded that for the sample without Gd doping, the ferrite was perfectly single phase spinel and as there was an increase in the Gd concentration, some un-indexed peak as secondary phase appeared. With the increase in Gd content, the lattice parameter also increased from 8.4645 Å to 8.4750 Å. In the XRD patterns of Al doped MnZn ferrite observed by Haralkar [184], the formation of cubic spinel ferrite structure was observed. It was observed that the lattice parameter decreased from 8.445 Å to 8.385 Å with increasing value of x due to the replacement of Fe^{3+}(0.67 Å) ions by Al^{3+}(0.51 Å). The value of X-ray density also decreased from 5.202 g/cm^3 to 4.989 g/cm^3 with increase in Al content. The crystallite size decreased from 19 nm to 11 nm with increase in Al content. From the study of Yadav et al. [182], the XRD pattern showed spinel structure without any impurity. Also, the graphs had very broad peaks indicating the ultrafine nature and small crystallite size of ferrites. The lattice parameter increased from 8.4052 Å to 8.4219 Å with increase in Sm^{3+} concentration. The crystallite size decreased from 12.9 nm to 8.7 nm. X-ray density also increased from 5.172 g/cm^3 to 6.295 g/cm^3. These all variations were because of the

Table 3
Values of Lattice parameter a (Å), Crystallite size D (nm), x-ray density $d_{x\text{-}ray}$ (g/cm^{-3}), Saturation magnetization M_s (emu/g), Coercivity H_c (Oe), absorption bands, Remanent magnetization M_r(emu/g) of MnZn ferrite nanoparticles by different synthesis techniques.

Cation distribution	Method of synthesis	Condition of synthesis		a (Å)	D (nm)	$d_{x\text{-}ray}$ (g/cm^{-3})	M_s (emu/g)	H_c (Oe)	Absorption band		M_r(emu/g)	References
		Sintering temperature	Composition						ν_1 (cm^{-1})	ν_2 (cm^{-1})		
$Mn_{0.5}Zn_{0.5}Fe_2O_4$	Co-precipitation method	973K	–	8.409	11.38	–	–	–	466.02	564.08	–	[203]
		1173K		8.444	39.02	–	–	–	424.94	519.78	–	
		1373K		8.483	67.42	–	–	–	485.59	586.88	–	
$Mn_xZn_{(1-x)}Fe_2O_4$	Novel combustion method	753K	x = 0.0–1.0	8.457–8.515	27–37	4.96–5.29	11–62	–	–	–	–	[259]
$Mn_xZn_{(1-x)}Fe_2O_4$	Combustion method	753K	x = 0.0	8.457	36.982	–	11.090	45.383	–	–	0.769	[77]
			x = 0.2	8.466	35.891	–	29.402	57.303		–	2.887	
			x = 0.4	8.478	34.630	–	41.017	42.824	–	–	3.415	
			x = 0.6	8.489	32.977	–	57.245	54.556	–	–	5.087	
			x = 0.8	8.515	31.288	–	61.574	74.826	–	–	6.335	
			x = 1.0	8.514	27.374	–	60.868	97.260	–	–	8.451	
$Mn_{(1-x)}Zn_xFe_2O_4$	Microwave- hydrothermal process	1173K	x = 0.0	8.302	–	5.12	53.33	153	–	–	21.70	[179]
			x = 0.2	8.315	–	5.35	59.91	169	–	–	24.55	
			x = 0.4	8.319	–	5.41	67.2	156	–	–	27.78	
			x = 0.6	8.322	–	5.48	78.26	167	–	–	29.58	
			x = 0.8	8.328	–	5.49	17.78	172	–	–	7.28	
			x = 1.0	8.331	–	4.98	10.74	149	–	–	4.36	
$Mn_{(1-x)}Zn_xFe_2O_4$	Glycine-nitrate auto-combustion method	–	x = 0.2	–	66.7	–	69	60	–	–	21.25	[204]
			x = 0.4	–	43.25	–	49.6	47	–	–	14	
			x = 0.6	–	44.5	–	48	40	–	–	12	
			x = 0.8	–	66.3	–	34	45	–	–	8	
$Mn_{0.5}Zn_{0.5}Fe_2O_4$	Chemical co-precipitation method	353K	–	8.439	7	5.21	–	–	–	–	–	[9]
		673K		8.439	11	5.21	–	–	–	–	–	
		773K		8.438	12	5.21	–	–	–	–	–	
		923K		8.431	13	5.23	–	–	–	–	–	
$Mn_{(1-x)}Zn_xFe_2O_4$	Sol gel method using gelatin	–	x = 0.2	8.4466	23	5.13	32.9	94.2	510	345	–	[186]
			x = 0.4	8.4625	37	5.15	37.6	85.6	520	350	–	
			x = 0.6	8.4321	40	5.25	25.9	67.1	526	354	–	
			x = 0.8	8.4164	44	5.32	43.7	80.7	540	355	–	
$Mn_{0.6}Zn_{0.4}Fe_2O_4$	Sol gel method	As prepared	–	–	11 ± 1	–	18.0	18.2	–	–	–	[192]
		623K		–	10 ± 2	–	22.4	45.6	–	–	–	
		873K		–	20 ± 2	–	3.9	30.3	–	–	–	
		1273K		–	78 ± 5	–	9.3	20.8	–	–	–	
		1473K		–	40 ± 5	–	35.0	54.5		–	–	
$Mn_{0.3}Zn_{0.7}Fe_2O_4$	Hydrothermal process	453K	–	8.432	14	5.27	27.7	–	–	–	–	[112]
$Mn_{(1-x)}Zn_xFe_2O_4$	Solid state reaction	1573K	x = 0.59	8.4749	–	4.96	36.22	44.63	–	–	–	[30]
			x = 0.61	8.4401	–	4.95	33.15	45.56	–	–	–	
			x = 0.65	8.4353	–	40.93	30.78	42.48	–	–	–	
$Mn_{0.85}Zn_{0.15}Ni_xFe_2O_4$	Sol-gel auto combustion method	1473K	x = 0.03	8.4555	12.611	–	120.89	0.123	–	–	–	[187]
			x = 0.06	8.4801	17.725	–	118.62	0.125	–	–	–	
			x = 0.09	8.5758	10.924	–	114.89	0.201	–	–	–	
			x = 0.12	8.5610	10.945	–	122.93	0.216	–	–	–	
			x = 0.15	8.4077	12.585	–	137.25	0.246	–	–	–	
$Mn_{0.5}Zn_{0.5}Sc_yFe_{2-y}O_4$	Solution combustion method	–	y = 0.00	8.434	20	–	24.6	68	538	358	3.01	[189]
			y = 0.01	8.422	22	–	22.84	58.92	540	361	5.37	
			y = 0.03	8.454	19.3	–	31.48	74.89	544	362	7.74	
			y = 0.05	8.431	20	–	23.45	84.32	540	361	6.28	
$Mn_{0.5}Zn_{0.4}Mg_{0.1}Fe_2O_4$	Solid state reaction	111423K	–	8.354	37	5.28	–	–	–	–	–	[190]
		111473K		8.336	45	5.31	–	–	–	–	–	
		111523K		8.322	38	5.34	–	–	–	–	–	

(*continued on next page*)

Table 3 (*continued*)

Cation distribution	Method of synthesis	Condition of synthesis		a (Å)	D (nm)	$d_{x\text{-}ray}$ (g/cm^{-3})	M_s (emu/g)	H_c (Oe)	Absorption band		M_r(emu/g)	References
		Sintering temperature	Composition						ν_1 (cm^{-1})	ν_2 (cm^{-1})		
$Mn_{0.55}Zn_{0.45}Gd_xFe_{2-x}O_4$	Double sintering ceramic technique	2023K	x = 0.00	8.465	–	5.15	51.2	–	–	–	–	[128]
			x = 0.01	8.468	–	5.16	46.4	–	–	–	–	
			x = 0.03	8.472	–	5.20	45.6	–	–	–	–	
			x = 0.05	8.472	–	5.22	44.7	–	–	–	–	
			x = 0.08	8.475	–	5.31	40.3	–	–	–	–	
$Mn_{0.5}Zn_{0.5}Al_xFe_{2-x}O_4$	Sol-gel auto combustion method	873K	x = 0.0	8.445	–	4.412	39	89	445	548	1.3	[184]
			x = 0.1	8.438	–	4.321	35	61	446	550	1.18	
			x = 0.2	8.421	–	4.198	29	59	452	550	0.9	
			x = 0.3	8.403	–	4.057	22.5	48	451	545	0.75	
			x = 0.4	8.391	–	3.996	17.5	35	452	538	0.54	
			x = 0.5	8.385	–	3.912	10	19	452	529	0.3	
$Mn_{0.5}Zn_{0.5}Sm_xFe_{2-x}O_4$	Chemical co-precipitation method	–	x = 0.0	8.4052	12.9	5.172	23.95	0	–	–	0	[182]
			x = 0.1	8.4118	10.2	5.275	31.72	0	–	–	0	
			x = 0.3	8.4216	9.9	5.875	37.75	180	–	–	3.55	
			x = 0.5	8.4219	8.7	6.295	42.10	250	–	–	8.50	
$Mn_{0.4}Zn_{0.6}In_yFe_{2-y}O_4$	Oxalate-co-precipitation technique	–	y = 0.000	8.391	14.6	5.315	–	–	–	–	–	[183]
			y = 0.035	8.393	15.5	5.368	–	–	–	–	–	
			y = 0.070	8.397	15.7	5.418	–	–	–	–	–	
			y = 0.100	8.418	15.9	5.445	–	–	–	–	–	

substitution of heavier atomic weight samarium with lower atomic weight iron. The XRD peaks of Indium doped Mn-Zn ferrite as studied by Kumar and group [183] showed the pure spinel phase of space group Fd3m. With the increase in Indium concentration, the XRD peaks shifted towards higher angle. This showed some lattice distortion in the cubic structure. The crystallite size increased from 14.6 nm to 15.9 nm with increasing doping concentration. The lattice constant increased from 8.391 Å to 8.418 Å. Also, the x-ray density increased from 5.315 g/cm^3 to 5.445 g/cm^3. XRD graphs of MnZn ferrite for various compositions and with Indium doping are shown in Fig. 11. The characteristics peaks match with the ferrite particles and show the phase group Fd3m and spinel structure having single phase. Hence, it is concluded that the MnZn ferrites have single phase spinel cubic structure with Fd3m phase group; however some distortion in the structure can be observed because of doping.

6.1.2. Morphological structure

Various techniques such as AFM, TEM, and SEM etc. are used to investigate the morphological structure of the ferrite nanoparticles. SEM is widely used for it but TEM is better than SEM because of poor resolution of SEM. AFM is a technique that can be used in different conditions like air, vacuum, liquid and moist conditions. Winiarska et al. [205] observed that the TEM gave core shell type structure formation. Mirsekari et al. [204] found from the SEM micrographs that the morphology of MnZn ferrite was porous, sponge like and agglomerated with an average particle size of 2 μm. Anwar et al. [9] observed from the SEM micrographs that the particles were spherical in shape. Gabal et al. [206] studies showed that TEM morphology showed very strong agglomeration of the cubic particles, having some particles in one line. From the SEM micrographs [192], mean grain diameter was observed 7.88±0.4 μm. In Phong's observation [112] of the TEM images showed that the ferrites had homogeneous structure and spherical in shape. Particles showed agglomeration due to slow particle growth. In the SEM analysis of the Ni doped ferrite done by Jalaiah [187], the presence of aggregates of small grains at the surface of the higher nickel containing samples was observed. In the TEM analysis done by Angadi et al. [189] the particles were lightly agglomerated due to the slow growth of particles during the preparation. The particle size of pure $Mn_{0.5}Zn_{0.5}Fe_2O_4$ was about 20 nm. The TEM images showed that the electron diffraction pattern consisted of concentric rings with spots over the rings showing that the samples were crystalline in nature. The particle size lies between 20 and 23 nm. From the SEM images [190], it was concluded that polyhedral morphology with nonuniform grains were displayed for both pure and doped MnZn ferrites. Pure MnZn ferrites sintered at 1150°C had average grain size of 2.10 μm having well defined grain boundaries and the sample sintered at 1200°C and 1250°C had grain size of 2.84 μm and 3.13 μm. In case of Mg doped ferrites, grain size increased with sintering temperature from 2.00 to 3.10 μm. From the TEM images [84], it was concluded that the molecules were spherical in shape and particles were aggregated. From the SEM analysis by Yadav et al. [182], it was observed that particle size increased with Sm content but bigger particles were formed by the agglomeration of ultra fine particles. The TEM images showed that all the particles were nearly spherical in shape and average particle size was 10–20 nm. SEM analysis [183] showed the uniform, spherical shaped and loosely agglomerated particles. The shape of the MnZn ferrites is usually spherical and having particle size in the 9–23 nm range. The SEM images of the pure MnZn ferrites are shown in Fig. 12 that shows spherical structure of the ferrite nanoparticles and in Fig. 13 SEM images shows elongated nature of the ferrite nanoparticles. Also, the TEM images of pure MnZn ferrite nanoparticles are shown in Fig. 14.

6.1.3. FT-IR analysis

FT-IR stands for Fourier transform Infrared, the method that is used for infrared spectroscopy. In infrared spectroscopy, IR radiation is

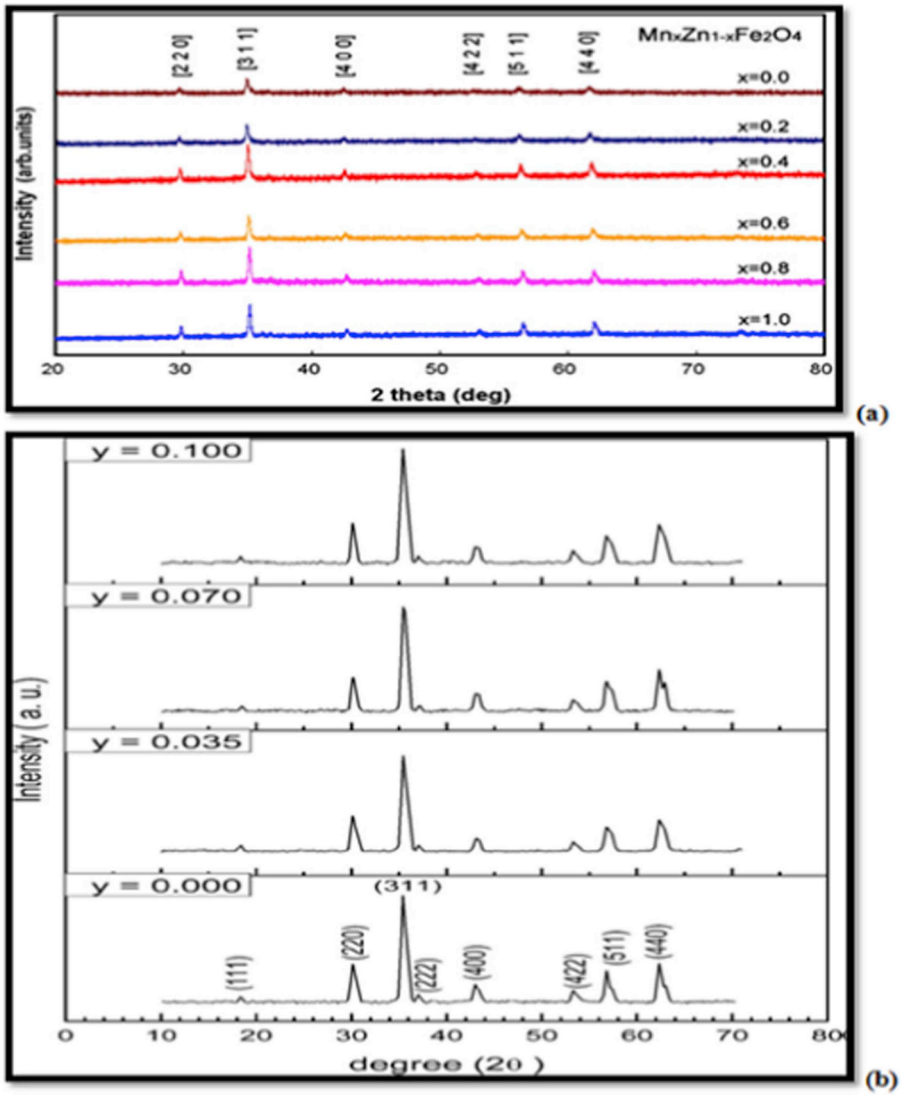

Fig. 11. (a) XRD powders pattern of synthesized Mn–Zn ferrite powders with x = 0.0, 0.2, 0.4, 0.6, 0.8, 1.0. The XRD pattern shows characteristic peaks of spinel structure and quality of pure phase (Reproduced by permission from Refs. [259], Licence No. 4646020803426, Copyright 2011, Elsevier), (b) X-ray diffraction pattern of MnZn ferrite with Indium substitution (Reproduced by permission from Refs. [183], Licence No. 4763520958822, Copyright 2016, Elsevier).

passed through a sample. Some of the infrared radiation is absorbed by the sample and some is passed through or transmitted. The resulting spectrum represents the molecular absorption and transmission, creating a molecular fingerprint of the sample. Islam et al. [128] recorded the FTIR spectra of MnZn ferrite nanoparticles in the range from 250 cm^{-1} to 4000 cm^{-1}. In the FTIR spectra [184], the value of the absorption band v_1 around 600 cm^{-1} remained almost constant whereas the value of absorption spectra v_2 around 400 cm^{-1} decreased from 548 cm^{-1} to 528 cm^{-1}. This is because of the difference in Fe^{3+}-O^{2-} distance for tetrahedral and octahedral sites. The absorption bands in the region 1200 cm^{-1}-1500 cm^{-1} correspond to NO_3^- ions, absorption band at 1700 cm^{-1} showed carboxyl group COO^- and at 2300 cm^{-1} correspond to hydrogen bonded O–H groups. In the FTIR spectra [189], two prominent absorption bands nearly at 540 cm^{-1}(v_1) and 360 cm^{-1}(v_2) observed were attributed to the tetrahedral and the octahedral complexes. The difference between these two values was due to the relative changes in bond length (Fe–O) at tetrahedral (A) sites and octahedral (B) sites.The FTIR spectra recorded by Gabal [206] in the range 600 cm^{-1}-200cm^{-1} showed high frequency band (v_1) increased with increasing Zn content due to vibrational spectra of metal ion-oxygen complex in the tetrahedral sites, while value of lower frequency band (v_2) due to vibration in the octahedral site, slightly changed. FTIR of all compounds showed the formation of spinel phase. Ciocarlan et al. [103] synthesized Mn ferrite along with Ni ferrite, Zn ferrite and Co ferrite and studied their various properties. Formation of spinel phase is observed from FT-IR spectra of all the compounds as shown in Fig. 17(b).

6.2. Power loss

MnZn ferrites are the magnetic materials with very low power loss so that they can be used in many electronic applications. Aiping et al. [123] synthesized MnZn ferrites using conventional ceramic processing technique and studied the effect of SnO_2 addition on the magnetic properties of the prepared ferrite. It was observed that there is an overall decrease in the loss factor with increase in SnO_2 concentration. Also, power loss and minimum power loss decreased with increase in the doping of SnO_2 as shown in Fig. 16 (c). Jalaiah et al. [187] studied structural, magnetic and electrical properties of nickel doped Mn–Zn spinel ferrite. The nickel substituted Mn–Zn ferrite $Mn_{0.85}Zn_{0.15}Ni_xFe_2O_4$ (x = 0.03, 0.06, 0.09, 0.12 and 0.15) were prepared using sol gel auto combustion method. The position of the

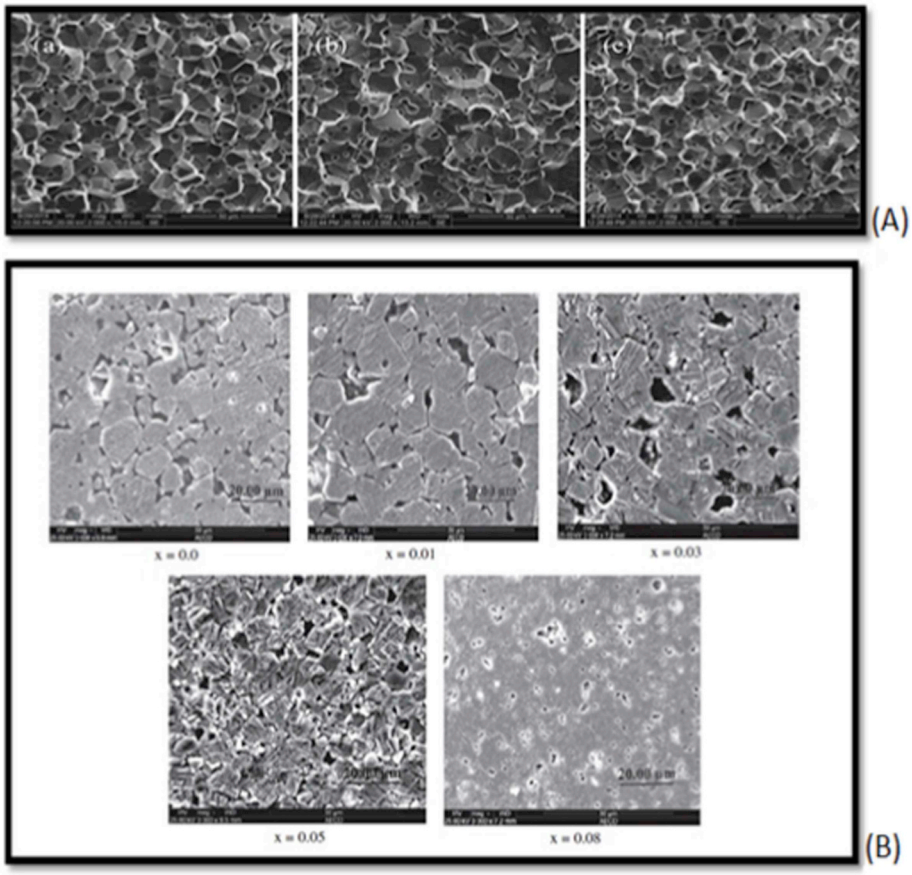

Fig. 12. (a) SEM images of Ti/Sn substituted MnZn ferrite, (Reproduced by permission from Ref. [125], Licence No. 4763511309362, Copyright 2015, Elsevier), (b) microstructure of MnZn ferrites with Gd concentration 0.0, 0.01, 0.03, 0.05 and 0.08 (Reproduced by permission from Refs. [128], Licence No. 4763520066588, Copyright 2013, Elsevier).

dielectric loss maxima shifted towards the lower frequency with increase in Ni concentration as dipole-dipole interaction becomes stronger at lower frequency causing hindrance to the rotation of the dipoles. The ac conductivity increased with increasing frequency. The room temperature conductivity of $Mn_{0.85}Zn_{0.15}Ni_xFe_2O_4$ (x = 0.03,0.06,0.09,0.12 and 0.15) ferrites was higher than pure spinel ferrite. Sun et al. [125] studied cation distribution and magnetic properties of Ti/Sn-substituted MnZn ferrites. Solid state reaction method was used to prepare Manganese–Zinc ferrites with composition $Mn_{0.782-x}Zn_{0.128}M_x^{4+}Fe_{2-2x}^{2+}O_4$ (x = 0; M = Ti, x = 0.04; M = Sn, x = 0.04). The core losses measured at 100 kHz and 200 mT showed that the core losses for all samples decreased firstly and then increased with increasing temperature further. The power loss for unsubstituted and Ti^{4+} sample was higher at room temperature. Also, temperature of minimum in $P_L \sim T$ curve shifts to lower temperature for Ti^{4+} and Sn^{4+} substituted samples. At low frequencies the there was power losses only due to eddy current loss P_e and hysteresis loss P_h. The P_h decreased with increasing temperature firstly up to 80 °C and then increased with further increase in temperature and it was minimum for Sn^{4+} doping. The P_e of all samples were relatively low and there was a slight change at low temperature but there was a sharp increase at high temperature as shown in Fig. 16 (a), (b). Wei et al. [129] studied effect of TiO_2 and Nb_2O_5 additives on the magnetic properties of cobalt-modified MnZn ferrites. Traditional ceramic process was used to prepare MnZn samples with composition ($Mn_{0.673}Zn_{0.246}Fe_{2.073}Co_{0.006}O_4$) by using Fe_2O_3, Mn_3O_4, ZnO and Co_2O_3 as the starting materials. The power loss vs. temperature plot showed that the power loss decreased firstly and then increased with an increase in temperature showing lowest loss point between 60 °C and 100 °C. Power loss reduced as the concentration of additives was increased. Also, both the hysteresis loss and the eddy current loss decreased with increase in concentration of additives and after reaching minima for concentration of TiO_2 and Nb_2O_5, 0.03 wt% and 0.02 wt% increased further. This is because as small amount of Ti^{4+} and Nb^{5+} ions were entered into the grains, it causes an increase in Fe^{2+} ions, which lead to positive K_1 values and decrease the hysteresis loss. Further increasing the dopant concentration cause excessive increase in Fe^{2+} ions, which make K_1 value more positive and increase the hysteresis loss. When the concentration of TiO_2 and Nb_2O_5 was less than 0.03 wt% and 0.02 wt%, the grain and grain boundary resistivity both increased and hence, the eddy current loss decreased as eddy current loss is inversely proportional to resistivity. Further increase in additives concentration decreased the resistivity, causing the eddy current loss to increase. Anwar et al. [9] studied the effect of sintering temperature on various structural, electrical and dielectric parameters of MnZn ferrites using the co-precipitation method for the synthesis of $Mn_{0.5}Zn_{0.5}Fe_2O_4$. The dielectric constant decreased very sharply in low frequency region and slowed down in high frequency region almost approaching to frequency independent nature. It exhibit dielectric dispersion. From the plot of loss tangent vs. frequency it was observed that the loss tangent decreased initially with increase in frequency and then showed a relaxation peak. It is observed from all this data that MnZn nanoferrites have very low power loss to be used suitably in making various electronic appliances.

6.3. Magnetic properties

Most common techniques for determining the magnetic properties of ferrite nanoparticles are VSM (vibrating sample magnetometer), magnetization hysteresis (M − H) loops and electron spin resonance (ESR) hysteresis loop measurements. We can calculate saturation magnetization, remenant magnetization and coercivity by using these characterization techniques.

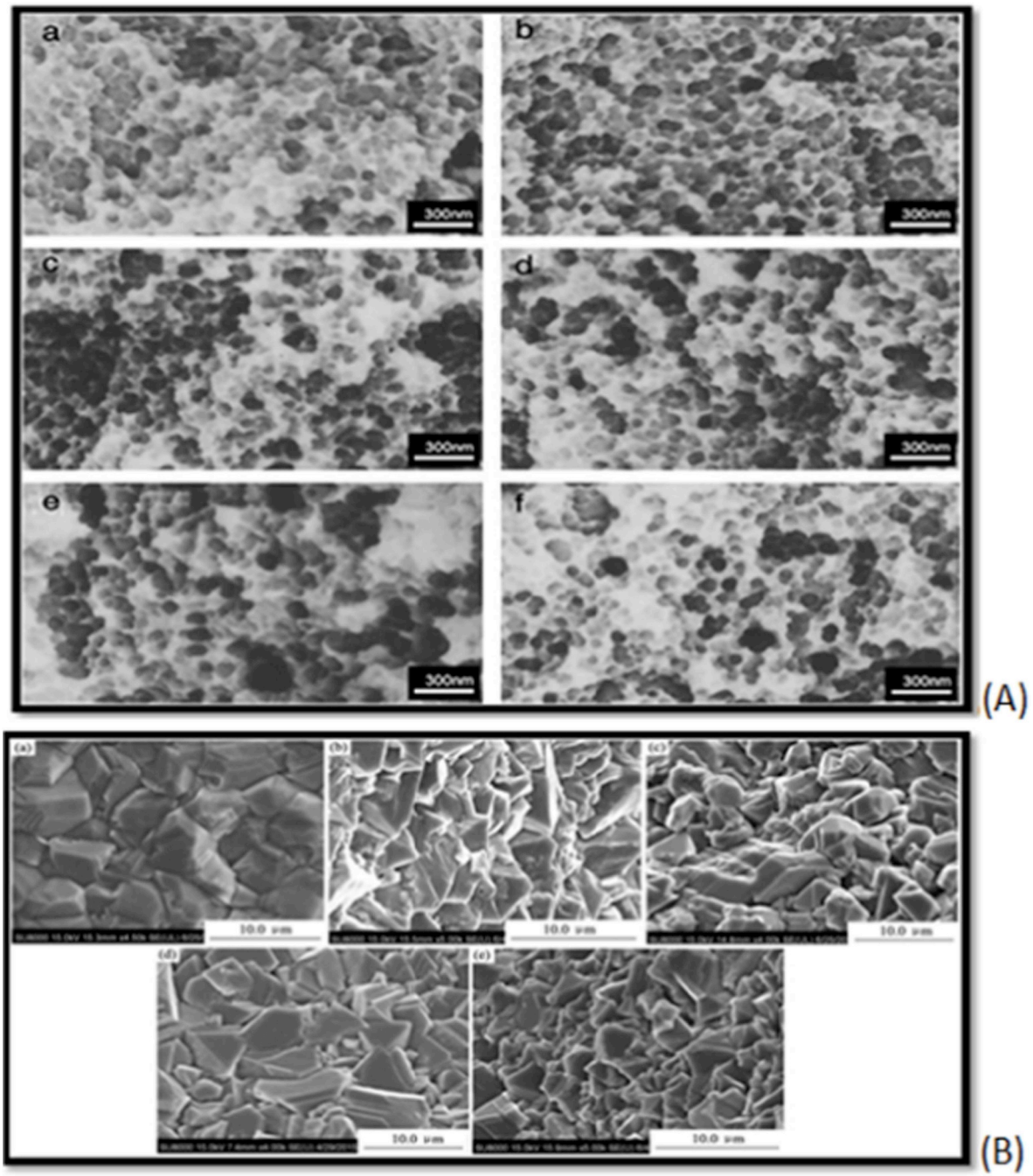

Fig. 13. (a)SEM micrographs show the as-synthesized $Mn_xZn_{1-x}Fe_2O_4$ powders: (a) x = 0.0, (b) x = 0.2, (c) x = 0.4, (d) x = 0.6, (e) x = 0.8, (f) x = 1.0 (Reproduced by permission from Ref. [259], Licence No. 4646020803426, Copyright 2011, Elsevier), (b) SEM images of MnZn ferrites doped with Sm and Gd (Reproduced by permission from Refs. [240], Licence No. 4763520638098, Copyright 2016, Elsevier).

6.3.1. Saturation magnetization

Saturation magnetization is the saturation value of magnetization of a ferromagnetic body. The inside of the magnetic body is normally divided into many number of domains, but as the external magnetic field increases, domain walls may move and magnetization may rotate within domains, so the magnetic body comes in single-domain state. The magnetization saturation is reached if the easy magnetization axis and the external magnetic field direction match and the value of the magnetization at this time is called the saturation magnetization. The value of this saturation magnetization of MnZn ferrites is high [141,162]in comparison to other ferrites. Syue et al. [188] observed the value of saturation magnetization increased from 11 to 62emu/g with increasing Mn^{2+} content and saturates further.The value of saturation magnetization remained in the range 11.090 emu/g to 60.868 emu/g [188] when combustion method is used without subsequent heat treatments. Praveena et al. [179] observed that the value of saturation magnetization (M_s) increased from 53.33 Am^2/Kg to 78.26 Am^2/Kg with increase in zinc content and then decreased to 10.74Am^2/kg if zinc content is further increased. From the hysteresis curves Mirsekari et al. [204] observed that the saturation magnetization decreased from 69 to 34 emu/g. Gabal et al. [186]observed the value of saturation magnetization M_s increased from 32.9emu/g to 37.6emu/g, then decreased to 25.9emu/g and again increased to 43.7emu/g.The value of saturation magnetization was found to be 27.7emu/g in Phong's [112] experiment showed the properties of super spin glass and supermagnetism behavior. The study by Zapata [30] showed that the M_s value decreased

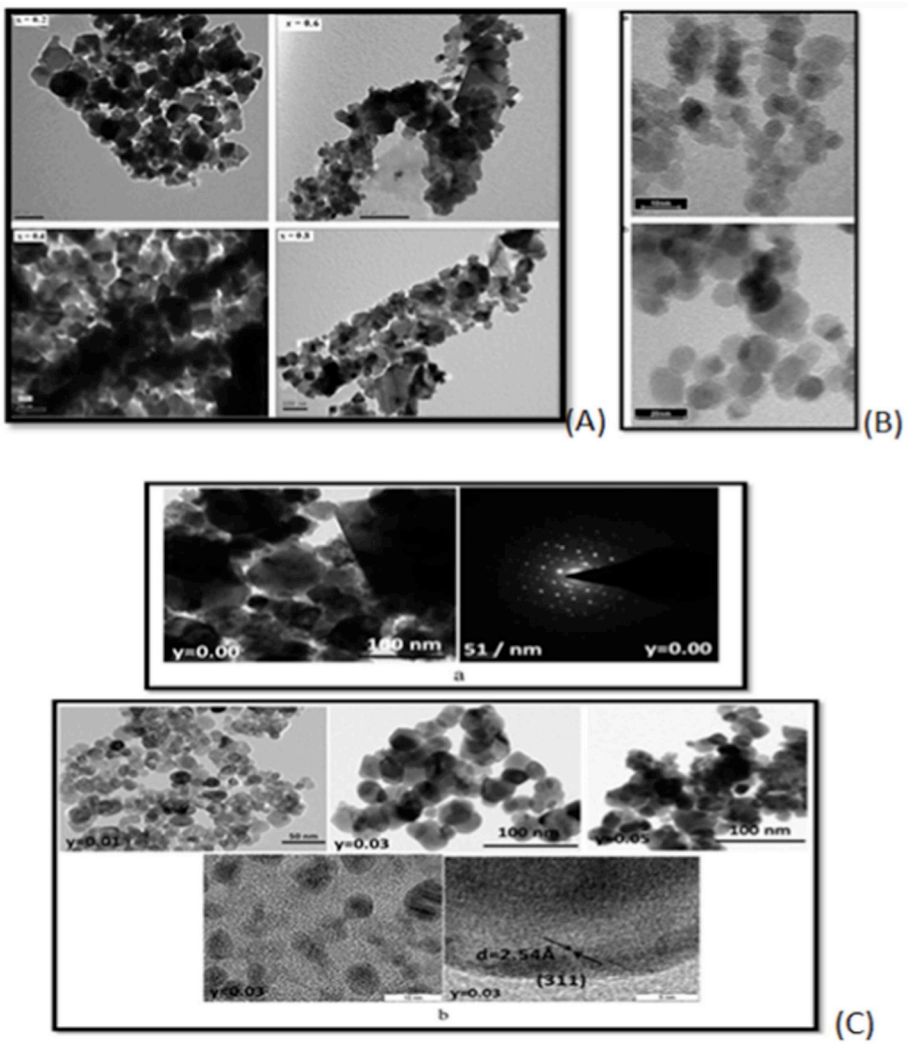

Fig. 14. TEM image of $Mn_{1-x}Zn_xFe_2O_4$ system prepared using gelatin method (Reproduced by permission from Refs. [186], Licence No: 4646030657048, Copyright 2012, Elsevier), (b)TEM micrographs of Mn–Zn ferrites annealed at 300 °C and 500 °C (Reproduced by permission from Ref. [165], Licence No: 4646030272206, Copyright 2011, Elsevier), (c) TEM and HRTEM images of Mn–Zn ferrite with Sc doping (Reproduced by permission from Ref. [189], Licence No: 4644680497245, Copyright 2017, Elsevier).

from 36.22emu/g to 30.78emu/g with increase in Zn concentration. This was due to the fact that increased Zn content decreased the ferric ions on the A sites and this reduced the A–B interaction. The saturation magnetization (M_s) [187] decreased firstly from 120.896emu/gm to 114.888emu/gm with increase in Ni concentration and then increased to 137.246emu/gm with further increase in Ni concentration as shown in Fig. 13. This decrease was due to the occupation of Ni^{2+} ions in octahedral B sites. Angadi et al. [171] observed from the M − H loops recorded by VSM that the variation of saturation magnetization(M_s) increased with increasing Sc^{3+} doping from 24.6emu/g to 31.48emu/g and then decreased further to 23.45emu/g. Hence, the Sc^{3+} doped Mn–Zn ferrites are useful for modern technological applications as well as low and high frequency applications. Islam et al. [128] observed that the value of saturation magnetization decreased from 51.2emu/gm to 40.3emu/gm with an increase in Gd content. By doping Al in pure MnZn ferrite [184] the saturation magnetization decreased with increase in Al content. Hysteresis loops measurements by Yadav et al. [182] showed that the value of saturation magnetization increased from 23.95emu/gm to 42.10emu/gm. Due to this, high value of magnetization MnZn ferrites are used in the field of power applications.

6.3.2. Remenant magnetization

Remanent magnetization is the value of magnetization that remains in the absence of an induced magnetic field. Mirshekari et al. [204] studied structural and magnetic properties of Mn–Zn ferrite. From the hysteresis curves, it was observed that remenant magnetization decreased from 21.25emu/g to 8 emu/g. Syue et al. [188] studied magnetic properties of MnZn ferrites and found that the value of remenant magnetization remained in the range 0.769 emu/g to 8.451emu/g and it was observed that it was lowest for pure zinc ferrite and highest for pure manganese ferrite. Praveena [179] studied magnetic properties of MnZn ferrite and found that remenant magnetization showed increase in value from 21.70Am^2/kg to 29.58Am^2/kg and then decreased to 4.36Am^2/kg with increasing x value as described in Table 3. Gabal et al. [186] showed that the remenant magnetization also increased from 5.5emu/g to 6.7emu/g firstly and then decreased to 3.6emu/g and again increased to 7.3emu/g. After doping Al [84,184] the remanence magnetization M_r varied from 0.5emu/g to 1.32emu/g with Al content. Yadav et al. [182]observed that remanence magnetization increased from 0emu/g to 8.50emu/gm with increasing value of Sm content from 0.0 to 0.5. Fig. 15 shows the results of VSM characterization of MnZn ferrite having high value of saturation magnetization and low coercivity.

6.3.3. Coercivity

The coercivity is also called as coercive field and coercive force. It is

defined as the ability of a ferromagnetic material to withstand an external magnetic field without demagnetizing it. In case of a ferromagnetic material, it is defined as the intensity of applied magnetic field that is required to reduce the magnetization to zero after the saturation state of the magnetization. The materials which have high coercivity are called hard materials and the materials with low value of coercivity are soft materials. The hard materials are used to make the permanent magnets and soft materials are used for making transformers, inductor cores and microwave devices. Praveena et al. [179] found the coercivity value varying in the range 0.0149Oe-0.0172Oe for $Mn_{1-x}Zn_xFe_2O_4$ (x = 0.0–1.0). From the hysteresis curves Mirsekari et al. [204] observed that the coercivity decreased from 60Oe to 45Oe with increasing x from 0.2 to 0.8. The coercivity as calculated by Gabal [186] showed decreasing trend. It decreased from 94.2Oe to 67.1Oe for x = 0.2–0.6 and then increased to 80.7Oe for x = 0.8. Phong et al. [112] studied the properties of MnZn ferrites and found that the coercivity was 130 Oe at 10K. Jalaiah et al. [187] observed from his experiment that the coercivity values of the $Mn_{0.85}Zn_{0.15}Ni_xFe_2O_4$ (x = 0.03, 0.06, 0.09, 0.12 and 0.15) samples increased with nickel concentration from 0.123Oe to 0.24Oe because of the decrease in the porosity with increasing dopant concentration. Also, the coercivity decreased from 87Oe to 11Oe with increasing Al^{3+} concentration [184]. The low value of coercivity of MnZn ferrite put these ferrites in the class of soft ferrites and these are used in applications like making transformer cores, microwave devices and inductors.

7. Applications of MnZn ferrites

Due to useful magnetic, electrical and optical properties of ferrite nanoparticles, researchers are taking interest in the synthesis of ferrite nanoparticles and making their use in a lot of applications that include medical field, information technology, antenna, microwave absorbing materials, biosensors and many electronic applications [207–216]. Many reviews are there about the synthesis, properties and applications of ferrites in biomedical [217–219], catalyst [220,221] and wastewater treatment [200,222–225]. MnZn ferrites have a broad area of applications due to high saturation magnetization [226], high initial permeability [50,227], low power loss [228]. The application area of MnZn ferrites include power applications [229–235], microwave devices [236], magnetic fluid [145,237], radar absorbing system, high frequency applications [238,239], bio-medical [240], water purification [241,242]etc. Use of MnZn ferrites in the field of power application attracted great attention in the research areas. From last many years the MnZn ferrites are synthesized to be used in power applications for making current convertors [227], power inductors with magnetic cores [130], electronic transformer cores [243], high frequency applications [143], electronics and communication [244].

7.1. Microwave devices

Ferrite nanoparticles have low electrical conductivity and low dielectric losses [245], so they can be used in microwave devices. MnZn ferrites are most suitable for their use in the microwave devices because of high permittivity, high resistivity, high stability, high value of saturation magnetization, high curie temperature with low eddy current and low magnetic losses [246,247]. Due to the use of ferrite nanomaterials, electronic devices can be mechanically hard, chemically stable and permit the materials to operate properly at a wide frequency range [248]. There are a lot of advantages of the use of MnZn ferrites in the microwave devices. There is a decrease in the emission of unwanted EM waves from the device and also it absorbs the incoming EM waves that may harm the microwave device. MnZn ferrites are used in microwave systems because of their low loss and high saturation magnetization. Wang et al. [249] synthesized MnZn ferrite nanoparticles and the result showed that because of high reflection loss and broad absorbing band in low frequency (10 MHz to 1 GHz) these ferrites can be used in electromagnetic microwave absorbing field.

7.2. Radar absorbing devices

The radiations emitting from radar results in the increase in electromagnetic radiation pollution in the environment. These radiations reduce the efficiency and performance of electronic instruments and thus decrease their lifetime and safety. As MnZn ferrite belongs to the class of soft ferrites having high electrochemical stability, high permeability, high saturation magnetization and low power losses, it is used in many electronic applications [65,79,128,167,199,209,210]. Ferrite nanoparticles can be used in the radar absorbing devices due to their high value of Curie temperature and temperature stability [250,251]. Also the ferrite nanoparticles are environmentally safe that make their use easier in the radar absorbing devices. The application of MnZn ferrites in radar absorbing system is also attracting the researchers. Praveena et al. [252] synthesized $Ni_{0.4}Zn_{0.2}Mn_{0.4}Fe_2O_4$nano ferrites for radar absorbing. The high value of Curie temperature indicated homogeneity and temperature stability. The EPR spectra showed reduction in the peak width and increase in relaxation with increase in sintering temperature. These all results showed that the ferrite nanoparticles can be used for radar absorbing from few MHz to 2 GHz and also these materials are environmentally safe.

7.3. Image based diagnostics

A one-pot thermal decomposition method was used to synthesize a series of Zn^{2+} doped nanoparticles of $(Zn_xMn_{1-x})Fe_2O_4$ and $(Zn_xFe_{1-x})Fe_2O_4$ (x = 0, 0.1, 0.2, 0.3, 0.4, and 0.8). By carefully controlling Zn^{2+} doping level, nanoparticles of size 15 nm with single crystallinity and size monodispersity (s < 5%) and having high magnetization value (175 emu/g) were obtained. The nanoparticles provided the large MRI contrast effects (r2 = 860 $mm^{-1}s^{-1}$) with an eight to fourteen fold increase in MRI contrast and a fourfold enhancement in hyperthermic effects compared to conventional iron oxide nanoparticles. This enhancement was significant for clinical purposes as the nanoparticle probe dosage level can be progressively lowered when using probes that have improved contrast enhancement effects. For $(Zn_xMn_{1-x})Fe_2O_4$ nanoparticles, Zn_{2+} ions mainly occupy tetrahedral sites of the spinel matrix which was confirmed by using extended X-ray absorption fine structure (EXAFS) analysis to examine the Zn and Fe K-edges. To detect small sized pathogenic targets precisely at an early stage, MRI contrast agents are often used to highlight those specific areas of interest. Due to high imaging contrast effects, magnetic nanoparticles can increase the difference between pathogenic targets and normal tissues via MRI. One of the most appropriate ways to increase the MR contrast effects is the optimization of saturation magnetization (Ms) that is directly related to the relaxivity coefficient (r2). The relaxivity coefficient (r2) is determined by a slope of R2 against nanoparticle concentration and often used as an indicator for contrast effects. The relaxivity coefficient (r2) of contrast agents can be tuned and further enhanced by engineering magnetic parameters [253].

7.4. Electronic devices

MnZn ferrite nanoparticles are used in making many electronic devices due to their enhanced electrical properties such as high value of resistivity, low ac conductivity, low power losses etc. Dobak et al. [105] studied miniaturization of components due to low loss MnZn ferrites. Also, Sun et al. [138] studied effect of ZrO_2 addition on the microstructure and various properties of MnZn ferrites and found that the optimal values of initial permeability (2322), saturation magnetization (522 mT) and power loss (386 kW/m^3) make it suitable for switch mode power supply applications. Due to suitable electrical and magnetic properties of the Sc^{3+} doped Mn–Zn ferrites, these were useful for modern technological application as well as for low and high frequency

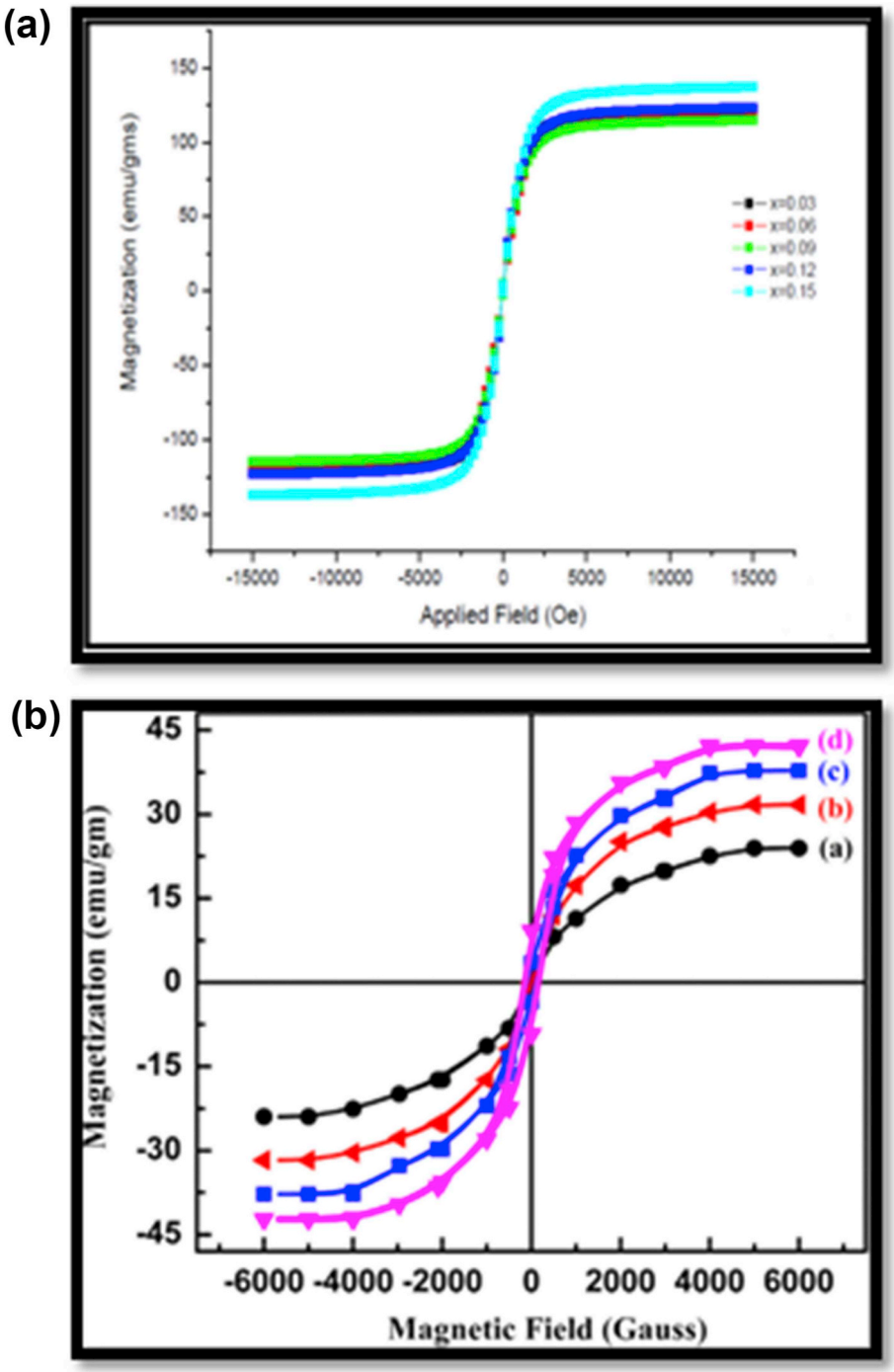

Fig. 15. (a) Magnetic hysteresis loops for $Mn_{0.85}Zn_{0.15}Ni_xFe_2O_4$ (x = 0.03, 0.06, 0.09, 0.12 and 0.15) (Reproduced by permission from Ref. [187], Licence No: 4656371369727, Copyright 2017, Elsevier), (b) Hysteresis loop of MnZn ferrite with Samarium doping where x is Sm concentration having (a) x = 0.0, (b) x = 0.1, (c) x = 0.3 and (d) x = 0.5 (Reproduced by permission from Refs. [182], Licence No. 4763520720419, Copyright 2015, Elsevier).

application. MnZn ferrites are also used to construct power inductors [254,255], wireless power transfer applications [256] and for making inductive components [39].

7.5. Telecommunication and others

One of the major use of MnZn ferrites is in telecommunication and high frequency applications [180]. MnZn ferrites have applications in the field of bio–medical and hyperthermia [112]. Hurtado et al. [257] synthesized MnZn ferrite along with activated carbon composite for use in bio–medical applications. MnZn ferrites can be used to make ferrofluid [182]due to high value of saturation magnetization. Arulmurugan et al. [76] synthesized Co–Zn and Mn–Zn ferrite nanoparticles and found that because of low Curie temperature and high value of thermomagnetic coefficient, these ferrites can be used for preparing temperature sensitive ferrofluid. Praveena et al. [258] synthesized Mn–Zn ferrite nanoparticles for high frequency applications. The ferrites had low power loss in frequency range 10Hz-1MHz. The constructed transformer with the ferrite material showed high efficiency and low surface temperature rise at frequency 1 MHz making it suitable for operating at high frequencies.

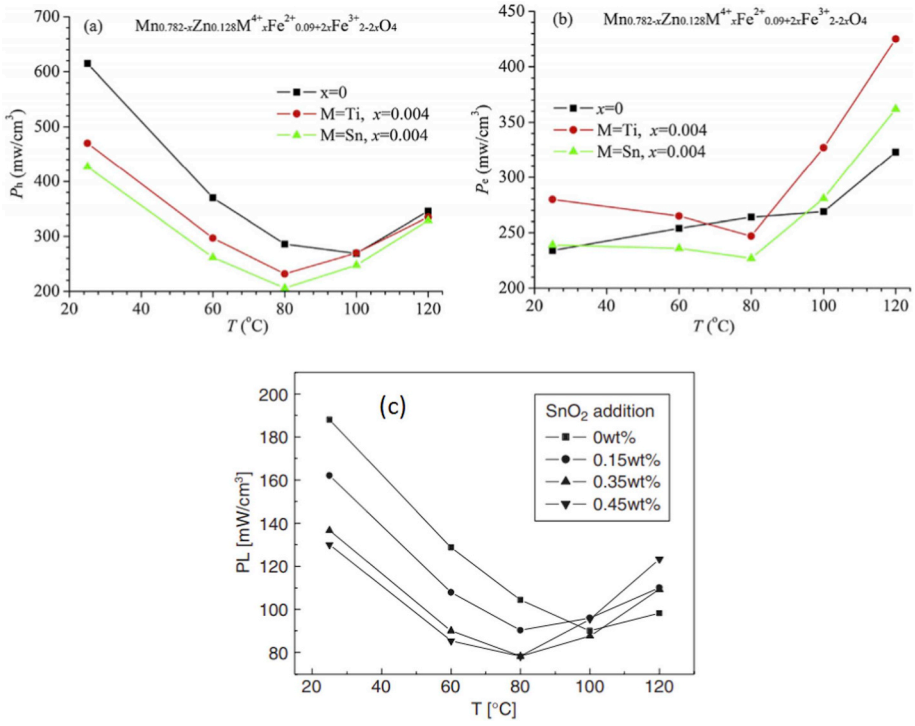

Fig. 16. (a-b) Temperature dependence of hysteresis loss and eddy current loss of MnZn ferrite (Reproduced by permission from Ref. [125], Licence No: 4763511309362, Copyright 2015, Elsevier), (c) Temperature dependance of power loss with SnO_2 addition (Reproduced by permission from Refs. [123], Licence No: 4763501423793, Copyright 2006, Elsevier).

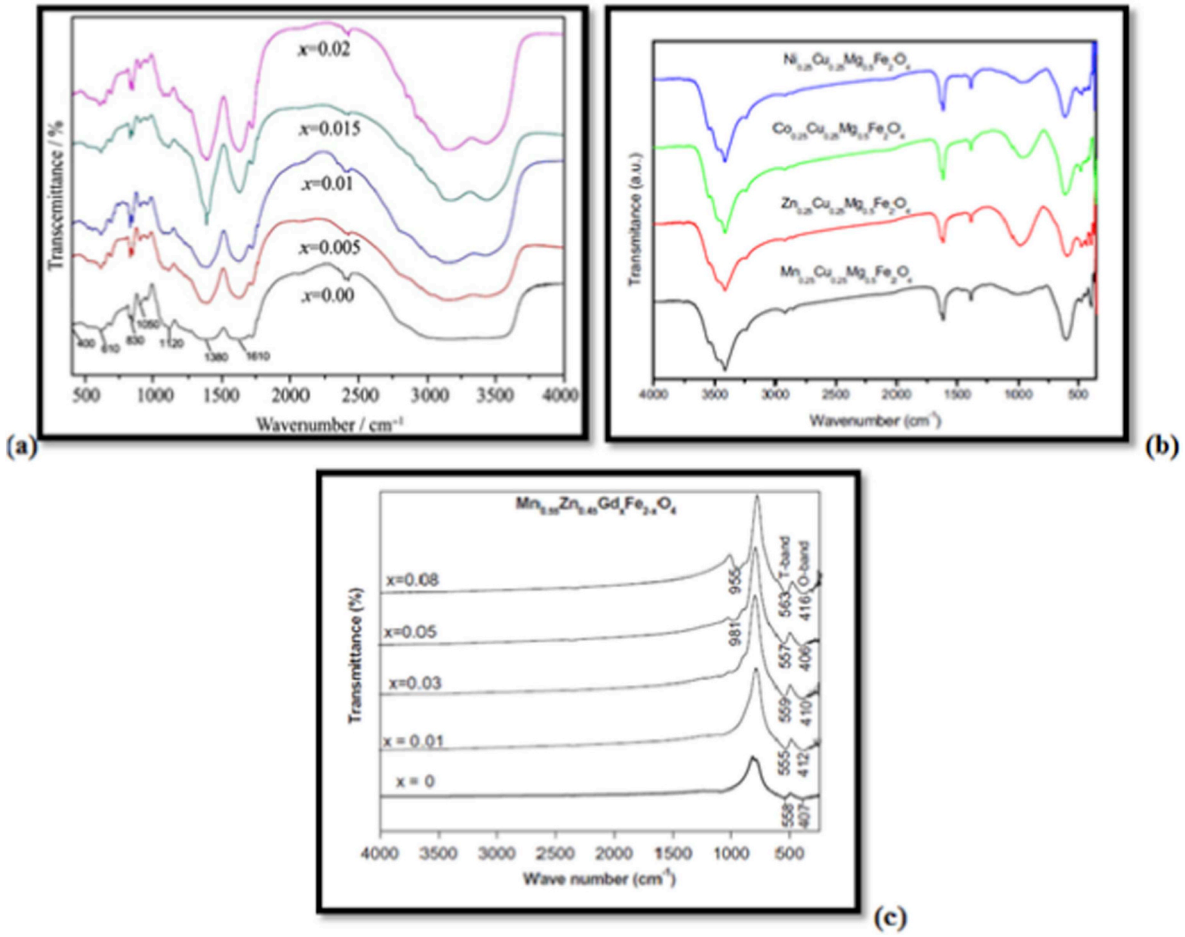

Fig. 17. (a) FT-IR spectra of MnZn ferrites with Sm and Gd doping (Reproduced by permission from Ref. [240], Licence No. 4763520638098, Copyright 2016, Elsevier), (b) FT-IR spectra of prepared nanoparticles (Reproduced by permission from Ref. [259], Licence No. 4763520231621, Copyright 2011, Elsevier), (c) FTIR spectra of MnZn ferrites with Gd doping (Reproduced by permission from Refs. [128], Licence No: 4763520066588, Copyright 2013, Elsevier).

7.6. MnZn ferrites for onging COVID-19 pandemics

As nanomaterials are making a global impact on healthcare and socioeconomic development so are the viruses during pandemics. Nanoparticles of MnZn have unique physical and chemical properties that have associated benefits in development of potential therapeutic drugs, nanomaterial based environment friendly antiviral sprays, drug delivery and to develop anti-viral surface coatings in home appliances. This is attributed to the fact that the choice of synthesis method provides size and charge tunability properties to the MnZn ferrites. The size tunablity ensures that large amount of drug can be delivered into anatomically privileged sites of the virus while charge tunability would facilitate entry of drug in to charged parts of the virus [260]. In addition, biosensors for the early detection of viral strains such the COVID 19 can also be developed with MnZn ferrites. For instance MnZn ferrites can readily be used to develop Giant magnetoresistance based sensors which have previously been used for virus detection [261].

8. Outlook

The synthesis of MnZn particles has increased in the last ten years and most progress can be seen in the year 2016. Due to the fascinating properties of MnZn ferrites among the class of soft ferrites like high value of saturation magnetization, low value of coercivity, high initial permeability, narrow size distribution of the ferrite particles, low remenant magnetization, the researchers are taking interest in the synthesis of these ferrites.The co-precipitation and sol-gel method are the best for getting the fine crystallite size among all synthesis techniques. The XRD pattern of the MnZn ferrites has characteristic peaks showing the cubic spinel phase having Fd3m phase group. The shape of the prepared ferrite is nearly spherical but some distortion may be observed after doping. FTIR spectra confirmed the spinel phase of the ferrite nanoparticles having tetrahedral and octahedral sites.The value of saturation magnetization is highest when we synthesize the MnZn ferrites with proper amount of nickel doping by using sol–gel auto combustion method. Also, for getting the low value of coercivity sol–gel method is preferred. Generally, MnZn ferrites have a lot of applications including biomedical field, electronic devices, for making radar absorbing materials, for making ferrofluids etc. For enhancing the applications and advantageous properties of MnZn ferrite nanoparticles, further studies are required.The electrical and magnetic properties of MnZn ferrites can be enhanced by doping other metals such as cobalt, zinc, magnesium to make them suitable for use in agricultural and electrical applications. In the context of use of nanoparticles in the pandemic outbreak, such as in the recent COVID-19, MnZn soft ferrites can play a significant role in the development of high contrast imaging dyes for viral strains in body fluids. Perhaps MnZn can also serve as a candidate nanomaterial for developing nanomaterial based medicines and therapeutics.

References

[1] M. Sugimoto, The past, present, and future of ferrites, J. Am. Ceram. Soc. 82 (2004) 269–280, https://doi.org/10.1111/j.1551-2916.1999.tb20058.x.

[2] Q. Song, Z.J. Zhang, Controlled synthesis and magnetic properties of bimagnetic spinel, J. Am. Chem. Soc. 134 (2012) 10182–10190, https://doi.org/10.1021/ja302856z.

[3] B. Skołyszewska, W. Tokarz, K. Przybylski, Z. Kakol, Preparation and magnetic properties of MgZn and MnZn ferrites, Physica C: Superconductivity and Its Applications 387 (2003) 290–294, https://doi.org/10.1016/S0921-4534(03)00696-8.

[4] C.M.B. Henderson, J.M. Charnock, D.A. Plant, Cation occupancies in Mg, Co, Ni, Zn, Al ferrite spinels: a multi-element EXAFS study, J. Phys. Condens. Matter 19 (2007), https://doi.org/10.1088/0953-8984/19/7/076214.

[5] T.R. Tatarchuk, M. Bououdina, N.D. Paliychuk, I.P. Yaremiy, V. V Moklyak, Structural characterization and antistructure modeling of cobalt- substituted zinc ferrites, J. Alloys Compd. 694 (2017) 777–791, https://doi.org/10.1016/j.jallcom.2016.10.067.

[6] N.M. Deraz, A. Alarifi, Journal of Analytical and Applied Pyrolysis Structural , morphological and magnetic properties of nano-crystalline zinc substituted cobalt ferrite system, J. Anal. Appl. Pyrol. 94 (2012) 41–47, https://doi.org/10.1016/j.jaap.2011.10.004.

[7] A. Namai, M. Yoshikiyo, K. Yamada, S. Sakurai, T. Goto, T. Yoshida, T. Miyazaki, M. Nakajima, T. Suemoto, H. Tokoro, S.I. Ohkoshi, Hard magnetic ferrite with a gigantic coercivity and high frequency millimetre wave rotation, Nat. Commun. 3 (2012) 1035–1036, https://doi.org/10.1038/ncomms2038.

[8] K.S. Martirosyan, N.S. Martirosyan, A.E. Chalykh, Structure and properties of hard-magnetic barium, strontium, and lead ferrites, Inorg. Mater. 39 (2003) 866–870, https://doi.org/10.1023/A:1025037716108.

[9] H. Anwar, A. Maqsood, Effect of sintering temperature on structural, electrical and dielectric parameters of Mn-Zn nano ferrites, Key Eng. Mater. 510–511 (2012) 163–170 https://doi.org/10.4028/www.scientific.net/kem.510-511.163.

[10] A.C.F.M. Costa, A.P.A. Diniz, A.G.B. de Melo, R.H.G.A. Kiminami, D.R. Cornejo, A.A. Costa, L. Gama, Ni-Zn-Sm nanopowder ferrites: morphological aspects and magnetic properties, J. Magn. Magn Mater. 320 (2008) 742–749, https://doi.org/10.1016/j.jmmm.2007.08.011.

[11] S.F. Mansour, O.M. Hemeda, M.A. Abdo, W.A. Nada, Improvement on the magnetic and dielectric behavior of hard/soft ferrite nanocomposites, J. Mol. Struct. 1152 (2018) 207–214, https://doi.org/10.1016/j.molstruc.2017.09.089.

[12] T. Sun, A. Borrasso, B. Liu, V. Dravid, Synthesis and characterization of nanocrystalline zinc manganese ferrite, J. Am. Ceram. Soc. 94 (2011) 1490–1495, https://doi.org/10.1111/j.1551-2916.2010.04265.x.

[13] A. Chauhan, R. Vaish, Magnetic material selection using multiple attribute decision making approach, Mater. Des. 36 (2012) 1–5, https://doi.org/10.1016/j.matdes.2011.11.021.

[14] W. Solano-Alvarez, E.J. Pickering, M.J. Peet, K.L. Moore, J. Jaiswal, A. Bevan, H.K.D.H. Bhadeshia, Soft novel form of white-etching matter and ductile failure of carbide-free bainitic steels under rolling contact stresses, Acta Mater. 121 (2016) 215–226, https://doi.org/10.1016/j.actamat.2016.09.012.

[15] J. Dho, E.K. Lee, J.Y. Park, N.H. Hur, Effects of the grain boundary on the coercivity of barium ferrite BaFe 12O19, J. Magn. Magn Mater. 285 (2005) 164–168, https://doi.org/10.1016/j.jmmm.2004.07.033.

[16] Q. Feng, X.H. Ma, Q.Z. Yan, C.C. Ge, Preparation of soft-agglomerated nano-sized ceramic powders by sol-gel combustion process, Mater. Sci. Eng. B: Solid-State Materials for Advanced Technology 162 (2009) 53–58, https://doi.org/10.1016/j.mseb.2009.02.007.

[17] N. Modaresi, R. Afzalzadeh, B. Aslibeiki, P. Kameli, A.G. Varzaneh, I. Orue, Magnetic properties of Zn x Fe 3 − x O 4 nanoparticles : A competition between the e ff ects of size and Zn doping level vol. 482, (2019), pp. 206–218.

[18] H.R. Kirchmayr, REVIEW ARTICLE Permanent magnets and hard magnetic materials, J. Appl. Phys. 29 (1996) 2763–2778.

[19] A. Chen, Y. Zhi, Y. Bao, Ceramic composites, J. Phys. Condens. Matter 6 (1999) 7921–7925, https://doi.org/10.1088/0953-8984/6/39/012.

[20] S. Torkian, A. Ghasemi, R.S. Razavi, Magnetic properties of hard-soft SrFe10Al2O19/Co0.8Ni0.2Fe2O4 ferrite synthesized by one-pot sol-gel auto-combustion, J. Magn. Magn Mater. 416 (2016) 408–416, https://doi.org/10.1016/j.jmmm.2016.05.050.

[21] F.J. Heiligtag, M. Niederberger, The fascinating world of nanoparticle research, Mater. Today 16 (2013) 262–271, https://doi.org/10.1016/j.mattod.2013.07.004.

[22] H. Stäblein, Hard ferrites and plastoferrites, Handb. Ferromagn. Mater. 3 (1982) 441–602, https://doi.org/10.1016/S1574-9304(05)80093-8.

[23] T.S. Chin, Permanent magnet films for applications in microelectromechanical systems, J. Magn. Magn Mater. 209 (2000) 75–79, https://doi.org/10.1016/S0304-8853(99)00649-6.

[24] S. He, H. Zhang, Y. Liu, F. Sun, X. Yu, X. Li, L. Zhang, L. Wang, K. Mao, G. Wang, Y. Lin, Z. Han, R. Sabirianov, H. Zeng, Maximizing specific loss power for magnetic hyperthermia by hard–soft mixed ferrites, Small 14 (2018) 1–9, https://doi.org/10.1002/smll.201800135.

[25] Haining Ji, Zhongwen Lan, Yu Zhong, Zhiyong Xu, Microstructure and temperature dependence of magnetic properties of MnZnTiSn ferrites for power applications, IEEE Trans. Magn. 46 (2009) 974–978, https://doi.org/10.1109/tmag.2009.2037954.

[26] C.I. Covaliu, D. Berger, C. Matei, L. Diamandescu, E. Vasile, C. Cristea, V. Ionita, H. Iovu, Magnetic nanoparticles coated with polysaccharide polymers for potential biomedical applications, J. Nanoparticle Res. 13 (2011) 6169–6180, https://doi.org/10.1007/s11051-011-0452-6.

[27] C.I. Covaliu, I. Jitaru, G. Paraschiv, E. Vasile, S.Ş. Biriş, L. Diamandescu, V. Ionita, H. Iovu, Core-shell hybrid nanomaterials based on CoFe2O4 particles coated with PVP or PEG biopolymers for applications in biomedicine, Powder Technol. 237 (2013) 415–426, https://doi.org/10.1016/j.powtec.2012.12.037.

[28] M.J. Carey, S. Maat, P. Rice, R.F.C. Farrow, R.F. Marks, A. Kellock, P. Nguyen, B.A. Gurney, Spin valves using insulating cobalt ferrite exchange-spring pinning layers, Appl. Phys. Lett. 81 (2002) 1044–1046, https://doi.org/10.1063/1.1494859.

[29] W.A. Kaczmarek, B.W. Ninham, Application of mechanochemistry in ferrite materials technology, J. Phys. IV (1997), https://doi.org/10.1051/jp4:1997106 C1-47-C1-48.

[30] A. Zapata, G. Herrera, Effect of zinc concentration on the microstructure and relaxation frequency of Mn-Zn ferrites synthesized by solid state reaction, Ceram. Int. 39 (2013) 7853–7860, https://doi.org/10.1016/j.ceramint.2013.03.046.

[31] G. Herrera, Domain wall dispersions: relaxation and resonance in Ni-Zn ferrite doped with V2 O3, J. Appl. Phys. 108 (2010) 3–8, https://doi.org/10.1063/1.3506716.

[32] S.C.Ó. Mathúna, T. O'Donnell, N. Wang, K. Rinne, Magnetics on silicon: an enabling technology for power supply on chip, IEEE Trans. Power Electron. 20

(2005) 585–592, https://doi.org/10.1109/TPEL.2005.846537.
[33] P. Mathur, A. Thakur, M. Singh, P HYSICAL J OURNAL nano-ferrite and characterization for high frequency 138 (2008) 133–138, https://doi.org/10.1051/epjap.
[34] P. Mathur, A. Thakur, M. Singh, IMPACT OF PROCESSING AND POLARIZATION ON DIELECTRIC BEHAVIOR OF $Ni_xMn_{0.4-x}Zn_{0.6}Fe_2O_4$SPINEL FERRITES, International Journal of Modern Physics B 23 (2009) 2523–2533, https://doi.org/10.1142/S0217979209052212.
[35] A. Hajalilou, S.A. Mazlan, A review on preparation techniques for synthesis of nanocrystalline soft magnetic ferrites and investigation on the effects of microstructure features on magnetic properties, Appl. Phys. Mater. Sci. Process 122 (2016), https://doi.org/10.1007/s00339-016-0217-2.
[36] V. Marghussian, Magnetic Properties of Nano-Glass Ceramics (2015), https://doi.org/10.1016/b978-0-323-35386-1.00004-9.
[37] V.S. Coker, N.D. Telling, G. Van Der Laan, R.A.D. Pattrick, C.I. Pearce, E. Arenholz, F. Tuna, R.E.P. Winpenny, J.R. Lloyd, Harnessing the extracellular bacterial production of nanoscale cobalt ferrite with exploitable magnetic properties, ACS Nano 3 (2009) 1922–1928, https://doi.org/10.1021/nn900293d.
[38] P.M. Tamhankar, A.M. Kulkarni, S.C. Watawe, Functionalization of cobalt ferrite nanoparticles with alginate coating for biocompatible applications, Mater. Sci. Appl. (2011) 1317–1321, https://doi.org/10.4236/msa.2011.29179 02.
[39] H. Zhao, C. Ragusa, C. Appino, O. De La Barriere, Y. Wang, F. Fiorillo, Energy losses in soft magnetic materials under symmetric and asymmetric induction waveforms, IEEE Trans. Power Electron. 34 (2019) 2655–2665, https://doi.org/10.1109/TPEL.2018.2837657.
[40] J. Füzer, M. Strečková, S. Dobák, Ďáková, P. Kollár, M. Fáberová, R. Bureš, Y. Osadchuk, P. Kurek, M. Vojtko, Innovative ferrite nanofibres reinforced soft magnetic composite with enhanced electrical resistivity, J. Alloys Compd. 753 (2018) 219–227, https://doi.org/10.1016/j.jallcom.2018.04.237.
[41] R. Justin Joseyphus, A. Narayanasamy, K. Shinoda, B. Jeyadevan, K. Tohji, Synthesis and magnetic properties of the size-controlled Mn-Zn ferrite nanoparticles by oxidation method, J. Phys. Chem. Solid. 67 (2006) 1510–1517, https://doi.org/10.1016/j.jpcs.2005.11.015.
[42] A.Z. Simões, C.S. Riccardi, M.L. Dos Santos, F.G. Garcia, E. Longo, J.A. Varela, Effect of annealing atmosphere on phase formation and electrical characteristics of bismuth ferrite thin films, Mater. Res. Bull. 44 (2009) 1747–1752, https://doi.org/10.1016/j.materresbull.2009.03.011.
[43] M. Pardavi-Horvath, Microwave applications of soft ferrites, J. Magn. Magn Mater. (2000), https://doi.org/10.1016/S0304-8853(00)00106-2.
[44] J. Töpfer, J. Mürbe, A. Angermann, S. Kracunovska, S. Barth, F. Bechtold, Soft ferrite materials for multilayer inductors, Int. J. Appl. Ceram. Technol. 3 (2006) 455–462, https://doi.org/10.1111/j.1744-7402.2006.02110.x.
[45] C. Miclea, C. Tanasoiu, C.F. Miclea, A. Gheorghiu, V. Tanasoiu, Soft ferrite materials for magnetic temperature transducers and applications, J. Magn. Magn Mater. 290–291 (2005) 1506–1509, https://doi.org/10.1016/j.jmmm.2004.11.561.
[46] S. Son, R. Swaminathan, M.E. McHenry, Structure and magnetic properties of rf thermally plasma synthesized Mn and Mn–Zn ferrite nanoparticles, J. Appl. Phys. 93 (2003) 7495–7497, https://doi.org/10.1063/1.1557953.
[47] Q.Y. Yan, R.J. Gambino, S. Sampath, Plasma-sprayed MnZn ferrites with insulated fine grains and increased resistivity for high-frequency applications, IEEE Trans. Magn. 40 (2004) 3346–3351, https://doi.org/10.1109/TMAG.2004.831658.
[48] G. Kogias, D. Holz, V. Zaspalis, New MnZn ferrites with high saturation flux density, J. Jpn. Soc. Powder Powder Metall. 61 (2014) S201–S203, https://doi.org/10.2497/jjspm.61.s201.
[49] Q. Xing, Z. Peng, C. Wang, Z. Fu, X. Fu, Doping effect of Y 3 ions on the microstructural and electromagnetic properties of MnZn ferrites, Phys. B Condens. Matter 407 (2012) 388–392, https://doi.org/10.1016/j.physb.2011.11.003.
[50] V. Babayan, N.E. Kazantseva, R. Moučka, I. Sapurina, Y.M. Spivak, V.A. Moshnikov, Combined effect of demagnetizing field and induced magnetic anisotropy on the magnetic properties of manganesezinc ferrite composites, J. Magn. Magn Mater. 324 (2012) 161–172, https://doi.org/10.1016/j.jmmm.2011.08.002.
[51] E.M. Mohammed, K.A. Malini, P. Kurian, M.R. Anantharaman, Modification of dielectric and mechanical properties of rubber ferrite composites containing manganese zinc ferrite, Mater. Res. Bull. 37 (2002) 753–768, https://doi.org/10.1016/S0025-5408(02)00690-6.
[52] S. Calvin, E.E. Carpenter, V.G. Harris, S.A. Morrison, Use of multiple-edge refinement of extended x-ray absorption fine structure to determine site occupancy in mixed ferrite nanoparticles, Appl. Phys. Lett. 81 (2002) 3828–3830, https://doi.org/10.1063/1.1520700.
[53] D.J. Fatemi, V.G. Harris, M.X. Chen, S.K. Malik, W.B. Yelon, G.J. Long, A. Mohan, X-ray absorption, neutron diffraction, and Mössbauer effect studies of MnZn–ferrite processed through high-energy ball milling, J. Appl. Phys. 85 (1999) 5172–5174, https://doi.org/10.1063/1.369114.
[54] A. Thakur, P. Mathur, M.Ã. Singh, Study of dielectric behaviour of Mn–Zn nano ferrites, Journal of Physics and Chemistry of Solids 68 (2007) 378–381, https://doi.org/10.1016/j.jpcs.2006.11.028.
[55] P. Mathur, A. Thakur, M. Singh, Low temperature processing of Mn-Zn nanoferrites, J. Mater. Sci. 42 (2007) 8189–8192, https://doi.org/10.1007/s10853-007-1690-y.
[56] J. Sláma, M. Šoka, A. Grusková, R. Dosoudil, V. Jančárik, J. Degmová, Magnetic properties of selected substituted spinel ferrites, J. Magn. Magn Mater. 326 (2013) 251–256, https://doi.org/10.1016/j.jmmm.2012.07.016.
[57] Y. Köseoğlu, M. Bay, M. Tan, A. Baykal, H. Sözeri, R. Topkaya, N. Akdoğan, Magnetic and dielectric properties of Mn0.2Ni 0.8Fe2O4 nanoparticles synthesized by PEG-assisted hydrothermal method, J. Nanoparticle Res. 13 (2011) 2235–2244, https://doi.org/10.1007/s11051-010-9982-6.
[58] J. Venturini, A.M. Tonelli, T.B. Wermuth, R.Y.S. Zampiva, S. Arcaro, A. Da Cas Viegas, C.P. Bergmann, Excess of cations in the sol-gel synthesis of cobalt ferrite (CoFe 2 O 4): A pathway to switching the inversion degree of spinels, J. Magn. Magn Mater. 482 (2019) 1–8, https://doi.org/10.1016/j.jmmm.2019.03.057.
[59] S. Bae, Y.K. Hong, J.J. Lee, J. Jalli, G.S. Abo, A. Lyle, B.C. Choi, G.W. Donohoe, High Q Ni-Zn-Cu Ferrite inductor for on-chip power module, IEEE Trans. Magn. 45 (2009) 4773–4776, https://doi.org/10.1109/TMAG.2009.2023856.
[60] D.L. Zhao, Q. Lv, Z.M. Shen, Fabrication and microwave absorbing properties of Ni-Zn spinel ferrites, J. Alloys Compd. 480 (2009) 634–638, https://doi.org/10.1016/j.jallcom.2009.01.130.
[61] H. Su, H. Zhang, X. Tang, X. Wei, Effects of calcining and sintering parameters on the magnetic properties of high-permeability MnZn ferrites, IEEE Trans. Magn. 41 (2005) 4225–4228, https://doi.org/10.1109/TMAG.2005.855327.
[62] H. Su, H. Zhang, X. Tang, Y. Jing, Z. Zhong, Complex permeability and permittivity spectra of polycrystalline Ni-Zn ferrite samples with different microstructures, J. Alloys Compd. 481 (2009) 841–844, https://doi.org/10.1016/j.jallcom.2009.03.133.
[63] S.-H. Park, W.-K. Ahn, J.-S. Kum, J.-K. Ji, K.-H. Kim, W.-M. Seong, Electromagnetic properties of dielectric and magnetic composite material for antenna, Electronic Materials Letters 5 (2009) 67–71, https://doi.org/10.3365/eml.2009.06.067.
[64] S. Son, M. Taheri, E. Carpenter, V.G. Harris, M.E. McHenry, Synthesis of ferrite and nickel ferrite nanoparticles using radio-frequency thermal plasma torch, J. Appl. Phys. 91 (2002) 7589–7591, https://doi.org/10.1063/1.1452705.
[65] T. Tsutaoka, Frequency dispersion of complex permeability in Mn–Zn and Ni–Zn spinel ferrites and their composite materials, J. Appl. Phys. 93 (2003) 2789–2796, https://doi.org/10.1063/1.1542651.
[66] H. Javed, F. Iqbal, P.O. Agboola, M.A. Khan, M.F. Warsi, I. Shakir, Structural, electrical and magnetic parameters evaluation of nanocrystalline rare earth Nd 3+ -substituted nickel-zinc spinel ferrite particles, Ceram. Int. 45 (2019) 11125–11130, https://doi.org/10.1016/j.ceramint.2019.02.176.
[67] R.A. Jasso-Terán, D.A. Cortés-Hernández, H.J. Sánchez-Fuentes, P.Y. Reyes-Rodríguez, L.E. de-León-Prado, J.C. Escobedo-Bocardo, J.M. Almanza-Robles, Synthesis, characterization and hemolysis studies of Zn(1 − x)CaxFe2O4 ferrites synthesized by sol-gel for hyperthermia treatment applications, J. Magn. Magn Mater. 427 (2017) 241–244, https://doi.org/10.1016/j.jmmm.2016.10.099.
[68] Y. Köseoǧlu, Structural and magnetic properties of Cr doped NiZn-ferrite nanoparticles prepared by surfactant assisted hydrothermal technique, Ceram. Int. 41 (2015) 6417–6423, https://doi.org/10.1016/j.ceramint.2015.01.079.
[69] J. Sánchez, D.A. Cortés-Hernández, M. Rodríguez-Reyes, Synthesis of TEG-coated cobalt-gallium ferrites: characterization and evaluation of their magnetic properties for biomedical devices, J. Alloys Compd. 781 (2019) 1040–1047, https://doi.org/10.1016/j.jallcom.2018.12.052.
[70] A.S. Džunuzović, N.I. Ilić, M.M. Vijatović Petrović, J.D. Bobić, B. Stojadinović, Z. Dohčević-Mitrović, B.D. Stojanović, Structure and properties of Ni-Zn ferrite obtained by auto-combustion method, J. Magn. Magn Mater. 374 (2015) 245–251, https://doi.org/10.1016/j.jmmm.2014.08.047.
[71] C.A. Palacio Gómez, J.J. McCoy, M.H. Weber, K.G. Lynn, Effect of Zn for Ni substitution on the properties of Nickel-Zinc ferrites as studied by low-energy implanted positrons, J. Magn. Magn Mater. 481 (2019) 93–99, https://doi.org/10.1016/j.jmmm.2019.03.002.
[72] J.S. Ghodake, R.C. Kambale, S.V. Salvi, S.R. Sawant, S.S. Suryavanshi, Electric properties of Co substituted Ni-Zn ferrites, J. Alloys Compd. 486 (2009) 830–834, https://doi.org/10.1016/j.jallcom.2009.07.075.
[73] S. Modak, M. Ammar, F. Mazaleyrat, S. Das, P.K. Chakrabarti, XRD, HRTEM and magnetic properties of mixed spinel nanocrystalline Ni-Zn-Cu-ferrite, J. Alloys Compd. 473 (2009) 15–19, https://doi.org/10.1016/j.jallcom.2008.06.020.
[74] A.C. Razzitte, S.E. Jacobo, W.G. Fano, Magnetic properties of MnZn ferrites prepared by soft chemical routes, J. Appl. Phys. 87 (2002) 6232–6234, https://doi.org/10.1063/1.372664.
[75] M. Li, H. Fang, H. Li, Y. Zhao, T. Li, H. Pang, J. Tang, X. Liu, Synthesis and characterization of MnZn ferrite nanoparticles with improved saturation magnetization, J. Supercond. Nov. Magnetism 30 (2017) 2275–2281, https://doi.org/10.1007/s10948-017-4013-9.
[76] R. Arulmurugan, B. Jeyadevan, G. Vaidyanathan, S. Sendhilnathan, Effect of zinc substitution on Co-Zn and Mn-Zn ferrite nanoparticles prepared by co-precipitation, J. Magn. Magn Mater. 288 (2005) 470–477, https://doi.org/10.1016/j.jmmm.2004.09.138.
[77] C.M. fu, M. ru Syue, fu J. Wei, C.W. Cheng, C.S. Chou, Synthesis of nanocrystalline Ni–Zn ferrites by combustion method with no postannealing route, J. Appl. Phys. 107 (2010) 585, https://doi.org/10.1063/1.3337689.
[78] A. Thakur, A. Chevalier, J.L. Mattei, P. Queffelec, Low-loss spinel nanoferrite with matching permeability and permittivity in the ultrahigh frequency range, J. Appl. Phys. 108 (2010) 1–5, https://doi.org/10.1063/1.3455875.
[79] M.A. Ahmed, N. Okasha, S.I. El-Dek, Preparation and characterization of nanometric Mn ferrite via different methods, Nanotechnology 19 (2008), https://doi.org/10.1088/0957-4484/19/6/065603.
[80] M. Stoia, L.B. Tudoran, P. Barvinschi, Nanosized zinc and magnesium ferrites obtained from PVA-metal nitrates' solutions, J. Therm. Anal. Calorim. 113 (2013) 11–19, https://doi.org/10.1007/s10973-012-2888-z.
[81] A. Angermann, J. Töpfer, K.L. Da Silva, K.D. Becker, Nanocrystalline Mn-Zn ferrites from mixed oxalates: synthesis, stability and magnetic properties, J. Alloys Compd. 508 (2010) 433–439, https://doi.org/10.1016/j.jallcom.2010.08.083.
[82] J. Jiang, L. Ai, L.C. Li, Synthesis and magnetic performance of polyaniline/Mn-Zn ferrite nanocomposites with intrinsic conductivity, J. Mater. Sci. 44 (2009)

1024–1028, https://doi.org/10.1007/s10853-008-3225-6.
[83] C. Aubery, C. Solans, M. Sanchez-Dominguez, Tuning high aqueous phase uptake in nonionic water-in-oil microemulsions for the synthesis of Mn-Zn ferrite nanoparticles: phase behavior, characterization, and nanoparticle synthesis, Langmuir 27 (2011) 14005–14013, https://doi.org/10.1021/la203125x.
[84] I. Szczygieł, K. Winiarska, Synthesis and characterization of manganese-zinc ferrite obtained by thermal decomposition from organic precursors, J. Therm. Anal. Calorim. 115 (2014) 471–477, https://doi.org/10.1007/s10973-013-3281-2.
[85] Y.Y. Meng, Z.W. Liu, H.C. Dai, H.Y. Yu, D.C. Zeng, S. Shukla, R.V. Ramanujan, Structure and magnetic properties of Mn(Zn)Fe 2-xRE xO 4 ferrite nano-powders synthesized by co-precipitation and refluxing method, Powder Technol. 229 (2012) 270–275, https://doi.org/10.1016/j.powtec.2012.06.050.
[86] A. Thakur, P. Thakur, J. Hsu, Structural , magnetic and electromagnetic characterization of in 3 + substituted Mn-Zn, Nanoferrites 228 (2014) 663–672, https://doi.org/10.1515/zpch-2014-0477.
[87] A. Thakur, P. Mathur, M. Singh, Controlling the Properties of Manganese-Zinc Ferrites by Substituting in 3 + and Al 3 + Ions vol. 221, (2007), pp. 837–845, https://doi.org/10.1524/zpch.2007.221.6.837.
[88] C. Rath, S. Anand, R.P. Das, K.K. Sahu, S.D. Kulkarni, S.K. Date, N.C. Mishra, Dependence on cation distribution of particle size, lattice parameter, and magnetic properties in nanosize Mn-Zn ferrite, J. Appl. Phys. 91 (2002) 2211–2215, https://doi.org/10.1063/1.1432474.
[89] K.K. Bamzai, G. Kour, B. Kaur, S.D. Kulkarni, Effect of cation distribution on structural and magnetic properties of Dy substituted magnesium ferrite, J. Magn. Magn Mater. 327 (2013) 159–166, https://doi.org/10.1016/j.jmmm.2012.09.013.
[90] S. Sakurai, S. Sasaki, M. Okube, H. Ohara, T. Toyoda, Cation distribution and valence state in Mn- Zn ferrite examined by synchrotron X-rays, Phys. B Condens. Matter 403 (2008) 3589–3595, https://doi.org/10.1016/j.physb.2008.05.035.
[91] T. Abbas, Y. Khan, M. Ahmad, S. Anwar, X-ray diffraction study of the cation distribution in the Mn-Zn-ferrites, Solid State Commun. 82 (1992) 701–703, https://doi.org/10.1016/0038-1098(92)90064-G.
[92] E. Veena Gopalan, I.A. Al-Omari, K.A. Malini, P.A. Joy, D. Sakthi Kumar, Y. Yoshida, M.R. Anantharaman, Impact of zinc substitution on the structural and magnetic properties of chemically derived nanosized manganese zinc mixed ferrites, J. Magn. Magn Mater. 321 (2009) 1092–1099, https://doi.org/10.1016/j.jmmm.2008.10.031.
[93] P. Papazoglou, E. Eleftheriou, V.T. Zaspalis, Low sintering temperature MnZn-ferrites for power applications in the frequency region of 400 kHz, J. Magn. Magn Mater. 296 (2006) 25–31, https://doi.org/10.1016/j.jmmm.2005.01.021.
[94] C. Beatrice, S. Dobák, V. Tsakaloudi, C. Ragusa, F. Fiorillo, L. Martino, V. Zaspalis, Magnetic loss, permeability, and anisotropy compensation in CoO-doped Mn-Zn ferrites, AIP Adv. 8 (2018), https://doi.org/10.1063/1.4993718.
[95] S. Thota, S.C. Kashyap, S.K. Sharma, V.R. Reddy, Cation distribution in Ni-substituted Mn0.5Zn0.5Fe2O4 nanoparticles: a Raman, Mössbauer, X-ray diffraction and electron spectroscopy study, Mater. Sci. Eng. B: Solid-State Materials for Advanced Technology 206 (2016) 69–78, https://doi.org/10.1016/j.mseb.2016.01.002.
[96] J. Azadmanjiri, Preparation of Mn-Zn ferrite nanoparticles from chemical sol-gel combustion method and the magnetic properties after sintering, J. Non-Cryst. Solids 353 (2007) 4170–4173, https://doi.org/10.1016/j.jnoncrysol.2007.06.046.
[97] K. Winiarska, I. Szczygieł, R. Klimkiewicz, Manganese-zinc ferrite synthesis by the sol-gel autocombustion method. Effect of the precursor on the ferrite's catalytic properties, Ind. Eng. Chem. Res. 52 (2013) 353–361, https://doi.org/10.1021/ie301658q.
[98] S. Yan, W. Ling, E. Zhou, Rapid synthesis of Mn0.65Zn0.35Fe2O 4/SiO2 homogeneous nanocomposites by modified sol-gel auto-combustion method, J. Cryst. Growth 273 (2004) 226–233, https://doi.org/10.1016/j.jcrysgro.2004.08.025.
[99] A. V Raut, R.S. Barkule, D.R. Shengule, K.M. Jadhav, Journal of Magnetism and Magnetic Materials Synthesis , structural investigation and magnetic properties of Zn 2 þ substituted cobalt ferrite nanoparticles prepared by the sol – gel autocombustion technique, J. Magn. Magn Mater. (2014) 87–92, https://doi.org/10.1016/j.jmmm.2014.01.039 358–359.
[100] T. Wegayehu, N. Murali, Y. Mulushoa, T. Arunamani, Studies of structural , morphological , electrical , and magnetic properties of Mg-substituted Co-ferrite materials synthesized using sol-gel autocombustion method, Physica B: Phys. Condens. Matter 523 (2017) 24–30, https://doi.org/10.1016/j.physb.2017.08.013.
[101] B.B.V.S.V. Prasad, K.V. Ramesh, A. Srinivas, Structural and Soft Magnetic Properties of Nickel-Substituted Co-zn Nanoferrites, (2018).
[102] F. Ameen Ramiza, S.K. Ajmal, M.B. Khan, A. Nasim, Y. Jamil, K. Kashif, S. Amira, Effect of UV radiations to control particle size of Mn-Zn spinel ferrite nano-particles, IOP Conference Series: Materials Science and Engineering, Institute of Physics Publishing, 2016, , https://doi.org/10.1088/1757-899X/146/1/012029.
[103] R.G. Ciocarlan, A. Pui, D. Gherca, C. Virlan, M. Dobromir, V. Nica, M.L. Craus, I.N. Gostin, O. Caltun, R. Hempelman, P. Cool, Quaternary M 0.25 Cu 0.25 Mg 0.5 Fe 2 O 4 (M = Ni, Zn, Co, Mn) ferrite oxides: synthesis, characterization and magnetic properties, Mater. Res. Bull. 81 (2016) 63–70, https://doi.org/10.1016/j.materresbull.2016.05.001.
[104] S. Irfan, M. Ajaz-Un-Nabi, Y. Jamil, N. Amin, Synthesis of Mn1-xZnxFe2O4 ferrite powder by co-precipitation method, IOP Conference Series: Materials Science and Engineering, Institute of Physics Publishing, 2014, , https://doi.org/10.1088/1757-899X/60/1/012048.
[105] S. Dobak, C. Beatrice, F. Fiorillo, V. Tsakaloudi, C. Ragusa, Magnetic loss decomposition in Co-Doped Mn-Zn ferrites, IEEE Magnetics Letters 10 (2019), https://doi.org/10.1109/LMAG.2018.2881108.
[106] R.P. Srivastava, O.P. Pandey, Head, Synthesis and Characterization of Mn-Zn Ferrite Nanomaterials by Chemical Co-precipitation Method Submitted by under the Guidance of, (2008).
[107] P. Mathur, A. Thakur, M. Singh, Effect of nanoparticles on the magnetic properties of Mn-Zn soft ferrite, J. Magn. Magn Mater. 320 (2008) 1364–1369, https://doi.org/10.1016/j.jmmm.2007.11.008.
[108] N.D. Kandpal, N. Sah, R. Loshali, R. Joshi, J. Prasad, Co-precipitation method of synthesis and characterization of iron oxide nanoparticles, J. Sci. Ind. Res. (India) 73 (2014) 87–90.
[109] F. Hua, C. Yin, H. Zhang, Q. Suo, X. Wang, H. Peng, Direct preparation of the nanocrystalline MnZn ferrites by using oxalate as precipitant, J. Mater. Sci. Chem. Eng. (2015) 23–29, https://doi.org/10.4236/msce.2015.312005 03.
[110] R.G. Welch, J. Neamtu, M.S. Rogalski, S.B. Palmer, Polycrystalline MnZn ferrite films prepared by pulsed laser deposition, Mater. Lett. 29 (1996) 199–203, https://doi.org/10.1016/S0167-577X(96)00146-2.
[111] M. Maisnam, S. Phanjoubam, Frequency dependence of electrical and magnetic properties of Li-Ni-Mn-Co ferrites, Solid State Commun. 152 (2012) 320–323, https://doi.org/10.1016/j.ssc.2011.11.019.
[112] P.T. Phong, P.H. Nam, D.H. Manh, D.K. Tung, I.J. Lee, N.X. Phuc, Studies of the magnetic properties and specific absorption of Mn0.3Zn0.7Fe2O4 nanoparticles, J. Electron. Mater. 44 (2015) 287–294, https://doi.org/10.1007/s11664-014-3463-0.
[113] D. Makovec, M. Drofenik, A. Žnidaršič, Hydrothermal synthesis of manganese zinc ferrite powders from oxides, J. Am. Ceram. Soc. 82 (2004) 1113–1120, https://doi.org/10.1111/j.1151-2916.1999.tb01884.x.
[114] M. Drofenik, D. Makovec, A. Znidarsic, Evolution of the MnZn-ferrite microstructure by applying of a thin liquid-phase film, WRTCS: X World Round Table Conference on Sintering, 2002 Belgrade; Serbia; 3-6 Sept. 2002.
[115] A. Thakur, M. Singh, Preparation and characterization of nanosize $Mn_{0.4}Zn_{0.6}Fe_2O_4$ ferrite by citrate precursor method, Ceram. Int. 29 (2003) 505–511, https://doi.org/10.1016/S0272-8842(02)00194-3.
[116] P. Mathur, A. Thakur, M. Singh, G. Harris, Preparation and Characterization of $Mn_{0.4}Ni_xZn_{0.6-x}Fe_2O_4$ Soft Spinel Ferrites for Low and High Frequency Applications by Citrate Precursor Method, Zeitschrift Für Physikalische Chemie 222 (2008) 621–633, https://doi.org/10.1524/zpch.2008.5265.
[117] P Mathur, A Thakur, M Singh, A Study of Nano-Structured Zn – Mn Soft Spinel Ferrites by the Citrate Precursor Method, Physica Scripta 77 (2008) 4045701, https://doi.org/10.1088/0031-8949/77/4/045701.
[118] G. Kogias, V.T. Zaspalis, Temperature stable MnZn ferrites for applications in the frequency region of 500 kHz, Ceram. Int. 42 (2016) 7639–7646, https://doi.org/10.1016/j.ceramint.2016.01.176.
[119] H. Mohseni, H. Shokrollahi, I. Sharifi, K. Gheisari, Magnetic and structural studies of the Mn-doped Mg-Zn ferrite nanoparticles synthesized by the glycine nitrate process, J. Magn. Magn Mater. 324 (2012) 3741–3747, https://doi.org/10.1016/j.jmmm.2012.06.009.
[120] A. Košak, D. Makovec, A. Žnidaršič, M. Drofenik, Preparation of MnZn-ferrite with microemulsion technique, J. Eur. Ceram. Soc. 24 (2004) 959–962, https://doi.org/10.1016/S0955-2219(03)00524-7.
[121] K.E. Sickafus, J.M. Wills, N.W. Grimes, Structure of spinel, J. Am. Ceram. Soc. 82 (2004) 3279–3292, https://doi.org/10.1111/j.1151-2916.1999.tb02241.x.
[122] S. Sanatombi, S. Sumitra, S. Ibetombi, Influence of sintering on the structural, electrical, and magnetic properties of Li–Ni–Mn–Zn ferrite synthesized by citrate precursor method, Iran. J. Sci. Technol. Trans. A-Science 42 (2018) 2397–2406, https://doi.org/10.1007/s40995-017-0405-8.
[123] H. Aiping, H. Huahui, F. Zekun, Effects of SnO2 addition on the magnetic properties of manganese zinc ferrites, J. Magn. Magn Mater. 301 (2006) 331–335, https://doi.org/10.1016/j.jmmm.2005.07.011.
[124] P. Andalib, Y. Chen, V.G. Harris, Concurrent core loss suppression and high permeability by introduction of highly insulating intergranular magnetic inclusions to MnZn ferrite, IEEE Magnetics Letters 9 (2017), https://doi.org/10.1109/LMAG.2017.2771391.
[125] K. Sun, G. Wu, B. Wang, Q. Zhong, Y. Yang, Z. Yu, C. Wu, P. Wei, X. Jiang, Z. Lan, Cation distribution and magnetic property of Ti/Sn-substituted manganese-zinc ferrites, J. Alloys Compd. 650 (2015) 363–369, https://doi.org/10.1016/j.jallcom.2015.07.258.
[126] S. Kumar, T. Shinde, P. Vasambekar, Engineering high permeability: Mn-Zn and Ni-Zn ferrites, Int. J. Appl. Ceram. Technol. 12 (2015) 851–859, https://doi.org/10.1111/ijac.12304.
[127] J. Kalarus, G. Kogias, D. Holz, V.T. Zaspalis, High permeability-high frequency stable MnZn ferrites, J. Magn. Magn Mater. 324 (2012) 2788–2794, https://doi.org/10.1016/j.jmmm.2012.04.011.
[128] R. Islam, M.A. Hakim, M.O. Rahman, H. Narayan Das, M.A. Mamun, Study of the structural, magnetic and electrical properties of Gd-substituted Mn-Zn mixed ferrites, J. Alloys Compd. 559 (2013) 174–180, https://doi.org/10.1016/j.jallcom.2012.12.080.
[129] Z. Wei, P. Zheng, L. Zheng, L. Shao, J. Hu, J. Zhou, H. Qin, Effect of TiO2and Nb2O5additives on the magnetic properties of cobalt-modified MnZn ferrites, J. Mater. Sci. Mater. Electron. 27 (2016) 6048–6052, https://doi.org/10.1007/s10854-016-4529-y.
[130] X. Fang, R. Wu, L. Peng, J.K.O. Sin, A novel silicon-embedded toroidal power inductor with magnetic core, IEEE Electron. Device Lett. 34 (2013) 292–294, https://doi.org/10.1109/LED.2012.2234077.
[131] A. Fujita, S. Gotoh, Temperature dependence of core loss in Co-substituted MnZn ferrites, J. Appl. Phys. 93 (2003) 7477–7479, https://doi.org/10.1063/1.1557952.
[132] S.F. Wang, Y.F. Hsu, C.H. Chen, Effects of Nb2O5, TiO2, SiO2, and CaO additions

on the loss characteristics of Mn-Zn Ferrite, J. Electroceram. 33 (2014) 172–179, https://doi.org/10.1007/s10832-014-9943-z.
[133] C.A. Baguley, U.K. Madawala, B. Carsten, The influence of remanence on magnetostrictive vibration and hysteresis in Mn-Zn ferrite cores, IEEE Trans. Magn. 48 (2012) 1844–1850, https://doi.org/10.1109/TMAG.2011.2174251.
[134] V. Tsakaloudi, G. Kogias, V.T. Zaspalis, Process and material parameters towards the design of fast firing cycles for high permeability MnZn ferrites, J. Alloys Compd. 588 (2014) 222–227, https://doi.org/10.1016/j.jallcom.2013.11.047.
[135] J. Töpfer, A. Angermann, Complex additive systems for Mn-Zn ferrites with low power loss, J. Appl. Phys. 117 (2015), https://doi.org/10.1063/1.4918692.
[136] M. Marracci, B. Tellini, Hysteresis losses of minor loops versus temperature in MnZn ferrite, IEEE Trans. Magn. 49 (2013) 2865–2869, https://doi.org/10.1109/TMAG.2012.2219877.
[137] H.H. Nien, C.K. Huang, M.Y. Wang, C.W. Lin, S.K. Changchien, Estimation of eddy-current loss for MnZn ferrite cores, Adv. Mater. Res. 382 (2011) 204–209 https://doi.org/10.4028/www.scientific.net/amr.382.204.
[138] B. Sun, F. Chen, W. Yang, H. Shen, D. Xie, Effects of nano-TiO2 and normal size TiO2 additions on the microstructure and magnetic properties of manganese-zinc power ferrites, J. Magn. Magn Mater. 349 (2014) 180–187, https://doi.org/10.1016/j.jmmm.2013.09.006.
[139] Y. Ying, Y. Gong, D. Liu, W. Li, J. Yu, L. Jiang, S. Che, Effect of MoO3Addition on the magnetic properties and complex impedance of Mn–Zn ferrites with high bsand high initial permeability, J. Supercond. Nov. Magnetism 30 (2017) 2129–2134, https://doi.org/10.1007/s10948-017-4002-z.
[140] N.S. Mitrović, B.S. Zlatkov, M.V. Nikolić, A.M. Maričić, O.S. Aleksić, S.R. Djukić, H. Danninger, Soft magnetic properties of MnZn ferrites prepared by powder injection moulding, Sci. Sinter. 44 (2012) 355–364, https://doi.org/10.2298/SOS1203355M.
[141] K. Parekh, R.V. Upadhyay, L. Belova, K.V. Rao, Ternary monodispersed Mn0.5Zn0.5Fe2O 4 ferrite nanoparticles: preparation and magnetic characterization, Nanotechnology 17 (2006) 5970–5975, https://doi.org/10.1088/0957-4484/17/24/011.
[142] A. Verma, M.I. Alam, R. Chatterjee, T.C. Goel, R.G. Mendiratta, Development of a new soft ferrite core for power applications, J. Magn. Magn Mater. 300 (2006) 500–505, https://doi.org/10.1016/j.jmmm.2005.05.040.
[143] J. Liu, Y. Mei, X. Li, G.Q. Lu, Effects of MnZn ferrite doping on magnetic and electrical properties of NiZnCu ferrite toroid cores for power applications, Proceedings - 2018 19th International Conference on Electronic Packaging Technology, ICEPT 2018, Institute of Electrical and Electronics Engineers Inc., 2018, pp. 965–968, , https://doi.org/10.1109/ICEPT.2018.8480541.
[144] V. Tsakaloudi, V. Zaspalis, Synthesis of a low loss Mn-Zn ferrite for power applications, J. Magn. Magn Mater. 400 (2016) 307–310, https://doi.org/10.1016/j.jmmm.2015.07.064.
[145] J. Patel, K. Parekh, R.V. Upadhyay, Performance of Mn-Zn ferrite magnetic fluid in a prototype distribution transformer under varying loading conditions, Int. J. Therm. Sci. 114 (2017) 64–71, https://doi.org/10.1016/j.ijthermalsci.2016.12.011.
[146] M. Latorre-Esteves, A. Cortés, M. Torres-Lugo, C. Rinaldi, Synthesis and characterization of carboxymethyl dextran-coated Mn/Zn ferrite for biomedical applications, J. Magn. Magn Mater. 321 (2009) 3061–3066, https://doi.org/10.1016/j.jmmm.2009.05.023.
[147] S. Nakagawa, S. Saito, T. Kamiki, S.-H. Kong, Mn–Zn spinel ferrite thin films prepared by high rate reactive facing targets sputtering, J. Appl. Phys. 93 (2003) 7996–7998, https://doi.org/10.1063/1.1555842.
[148] J. Stergar, Z. Jirák, P. Veverka, L. Kubí, T. Vrba, J. Kuličková, K. Kní, F. Porcher, J. Kohout, J. Stergar, Z. Jirák, P. Veverka, L. Kubíčková, T. Vrba, Mn-Zn ferrite nanoparticles coated with mesoporous silica as core material for heat-triggered release of therapeutic agents, J. Magn. Magn Mater. (2018), https://doi.org/10.1016/j.jmmm.2018.11.020.
[149] S. Liu, L. Wang, K. Chou, Synthesis of metal-doped Mn-Zn ferrite from the leaching solutions of vanadium slag using hydrothermal method, Journal of Magnetism and Magnetic Materials 449 (2018) 49–54, https://doi.org/10.1016/j.jmmm.2017.10.001.
[150] P.T. Phong, P.H. Nam, N.X. Phuc, B.T. Huy, L.T. Lu, D.H. Manh, I. Lee, Effect of Zinc Concentration on the Structural , Optical , and Magnetic Properties of Mixed Co-zn Ferrites Nanoparticles Synthesized by Low- Temperature Hydrothermal Method, Metallurgical and Materials Transactions A 50 (2019), https://doi.org/10.1007/s11661-018-5096-z.
[151] J. Feng, R. Xiong, Y. Liu, F. Su, X. Zhang, Preparation of cobalt substituted zinc ferrite nanopowders via auto- combustion route : an investigation to their structural and magnetic properties, J. Mater. Sci. Mater. Electron. (2018), https://doi.org/10.1007/s10854-018-9950-y 0.
[152] M. Augustin, T. Balu, Synthesis and characterization of metal (Mn,Zn) ferrite magnetic nanoparticles, Materials Today: Proceedings, Elsevier Ltd, 2015, pp. 923–927, , https://doi.org/10.1016/j.matpr.2015.06.010.
[153] Ö. Yavuz, M.K. Ram, M. Aldissi, P. Poddar, S. Hariharan, Synthesis and the physical properties of MnZn ferrite and NiMnZn ferrite-polyaniline nanocomposite particles, J. Mater. Chem. 15 (2005) 810–817, https://doi.org/10.1039/b408165j.
[154] M. Lauda, J. Füzer, P. Kollár, M. Strečková, R. Bureš, J. Kováč, M. Batkova, I. Batko, Magnetic properties and loss separation in FeSi/MnZnFe2O4soft magnetic composites, J. Magn. Magn Mater. 411 (2016) 12–17, https://doi.org/10.1016/j.jmmm.2016.03.051.
[155] L. Zhenyu, X. Guangliang, Z. Yalin, Microwave assisted low temperature synthesis of MnZn ferrite nanoparticles, Nanoscale Research Letters 2 (2007) 40–43, https://doi.org/10.1007/s11671-006-9027-3.
[156] H.H. Liu, J.C. Wang, C. Hsu, Deposition of nanoscale films on the nanopore-arrayed template by an in-situ spinning-precipitated technique, Synthesis and Reactivity in Inorganic, Metal-Organic and, Nano-Metal Chemistry 38 (2008) 152–155, https://doi.org/10.1080/15533170801926010.
[157] S. Okamoto, Y. Narumiya, T. Yamaguchi, Molten-salt synthesis of flaky MnZn-ferrite powder for electromagnetic shielding applications, Ceram. Int. 12 (1986) 209–212, https://doi.org/10.1016/0272-8842(86)90046-5.
[158] K. Hoshi, H. Kenmochi, T. Fukunaga, S. Furusawa, H. Sakurai, Synthesis of MnZn-ferrite using sintering aids, Key Eng. Mater. 534 (2013) 26–30 https://doi.org/10.4028/www.scientific.net/kem.534.26.
[159] J. Ren, Z. Zhang, Y. Zhong, J. Zhang, Z. Ren, Y. Liu, Z. Zhang, Y. Zhong, J. Zhang, Z. Ren, Y. Liu, Tuning the Structural and Magnetic Properties of MnZn Nano-Ferrites Synthesized under a High Magnetic Field, (2019).
[160] F. Arteaga-cardona, U. Pal, J. María, P. De, M. Mendoza-álvarez, U. Salazar-kuri, M.Á. Méndez-rojas, Journal of Magnetism and Magnetic Materials Tuning Magnetic and Structural Properties of MnFe 2 O 4 Nanostructures by Systematic Introduction of Transition Metal Ions M 2 + (M = Zn , Fe , Ni , Co), (2019), p. 490.
[161] Z. Duan, X. Tao, J. Xu, Characterization of as-deposited and sintered Mn0.5Zn0.5Fe2O4 films formed by sol-gel, Ferroelectrics 528 (2018) 131–138, https://doi.org/10.1080/00150193.2018.1449440.
[162] I.C. Masthoff, A. Gutsche, H. Nirschl, G. Garnweitner, Oriented attachment of ultra-small Mn(1-x)ZnxFe2O4 nanoparticles during the non-aqueous sol-gel synthesis, CrystEngComm 17 (2015) 2464–2470, https://doi.org/10.1039/c4ce02068e.
[163] D. Liu, S. Gao, R. Jin, F. Wang, X. Chu, T. Gao, Y. Wang, Enhanced soft magnetic properties of iron powders through coating MnZn ferrite by one-step sol–gel synthesis, Chin. Phys. B 28 (2019) 057503, , https://doi.org/10.1088/1674-1056/28/5/057503.
[164] R. Jabbar, S.H. Sabeeh, A.M. Hameed, Journal of Magnetism and Magnetic Materials Structural , Dielectric and Magnetic Properties of Mn + 2 Doped Cobalt Ferrite Nanoparticles, (2020), p. 494.
[165] J. Töpfer, A. Angermann, Nanocrystalline magnetite and Mn-Zn ferrite particles via the polyol process: synthesis and magnetic properties, Mater. Chem. Phys. 129 (2011) 337–342, https://doi.org/10.1016/j.matchemphys.2011.04.025.
[166] P. Mathur, A. Thakur, M. Singh, Processing of high density manganese zinc nanoferrites by Co-precipitation, Method 221 (2007) 887–895, https://doi.org/10.1524/zpch.2007.221.7.887.
[167] P. Mathur, A. Thakur, M. Singh, STUDY OF LOW-TEMPERATURE SINTERED NANO-CRYSTALLITE Mn-Cu-Zn FERRITE PREPARED BY CO-PRECIPITATION METHOD, Modern Physics Letters B 21 (2007) 1425–1430, https://doi.org/10.1142/S0217984907013651.
[168] L. Li, Z. Lan, Z. Yu, K. Sun, Z. Xu, Effects of Co-substitution on wide temperature ranging characteristic of electromagnetic properties in MnZn ferrites, J. Alloys Compd. 476 (2009) 755–759, https://doi.org/10.1016/j.jallcom.2008.09.101.
[169] X.L. Fu, Q.K. Xing, Z.J. Peng, C.B. Wang, Z.Q. Fu, L.H. Qi, H.Z. Miao, MICROSTRUCTURAL AND ELECTROMAGNETIC PROPERTIES OF Mn – Zn FERRITES WITH LOW MELTING-POINT NONMAGNETIC Sb 3+ IONS, Int. J. Mod. Phys. B 27 (2012) 1350003, https://doi.org/10.1142/s0217979213500033.
[170] M.M. Haque, M. Huq, M.A. Hakim, Densification, magnetic and dielectric behaviour of Cu-substituted Mg-Zn ferrites, Mater. Chem. Phys. 112 (2008) 580–586, https://doi.org/10.1016/j.matchemphys.2008.05.097.
[171] V. Jagadeesha Angadi, B. Rudraswamy, K. Sadhana, S.R. Murthy, K. Praveena, Effect of Sm3+-Gd3+ on structural, electrical and magnetic properties of Mn-Zn ferrites synthesized via combustion route, J. Alloys Compd. 656 (2016) 5–12, https://doi.org/10.1016/j.jallcom.2015.09.222.
[172] V.T. Zaspalis, E. Antoniadis, E. Papazoglou, V. Tsakaloudi, L. Nalbandian, C.A. Sikalidis, The effect of Nb2O5 dopant on the structural and magnetic properties of MnZn-ferrites, J. Magn. Magn Mater. 250 (2002) 98–109, https://doi.org/10.1016/S0304-8853(02)00367-0.
[173] J. Xiang, X. Shen, Y. Zhu, Effects of Ce3+ doping on the structure and magnetic properties of Mn-Zn ferrite fibers, Rare Met. 28 (2009) 151–155, https://doi.org/10.1007/s12598-009-0030-6.
[174] M. Rozman, M. Drofenik, Hydrothermal synthesis of manganese zinc ferrites, J. Am. Ceram. Soc. 78 (1995) 2449–2455, https://doi.org/10.1111/j.1151-2916.1995.tb08684.x.
[175] D.K. Agrawal, Microwave processing of ceramics, Curr. Opin. Solid State Mater. Sci. 3 (1998) 480–485, https://doi.org/10.1016/S1359-0286(98)80011-9.
[176] A. Manikandan, L.J. Kennedy, M. Bououdina, J.J. Vijaya, Journal of Magnetism and Magnetic Materials Synthesis , optical and magnetic properties of pure and Co-doped ZnFe 2 O 4 nanoparticles by microwave combustion method, J. Magn. Magn Mater. 349 (2014) 249–258, https://doi.org/10.1016/j.jmmm.2013.09.013.
[177] A. Manikandan, J.J. Vijaya, M. Sundararajan, C. Meganathan, L.J. Kennedy, M. Bououdina, Optical and magnetic properties of Mg-doped $ZnFe_2O_4$ nanoparticles prepared by rapid microwave combustion method, Superlattice. Microst. 64 (2013) 118–131, https://doi.org/10.1016/j.spmi.2013.09.021.
[178] G. Yang, S.-J. Park, Conventional and microwave hydrothermal synthesis and application of functional materials: a review, Materials 12 (2019) 1177, https://doi.org/10.3390/ma12071177.
[179] K. Praveena, K. Sadhana, H.S. Virk, Structural and magnetic properties of Mn-Zn ferrites synthesized by microwave-hydrothermal process, Solid State Phenom. 232 (2015) 45–64 https://doi.org/10.4028/www.scientific.net/ssp.232.45.
[180] A. Goldman, A. Laing, A NEW PROCESS for COPRECIPITATION of FERRITES, Journal de Physique Colloques 38 (1977) C1-297–C1-301, https://doi.org/10.1051/jphyscol:1977162ff. ffjpa-00217022.
[181] P. Thakur, R. Sharma, M. Kumar, S.C. Katyal, P.B. Barman, V. Sharma, P. Sharma, Structural, morphological, magnetic and optical study of co-precipitated Nd 3+

doped Mn-Zn ferrite nanoparticles, J. Magn. Magn Mater. 479 (2019) 317–325, https://doi.org/10.1016/j.jmmm.2019.02.048.
[182] N. Yadav, A. Kumar, P.S. Rana, D.S. Rana, M. Arora, R.P. Pant, Finite size effect on Sm^{3+} doped $Mn_{0.5}Zn_{0.5}Sm_xFe_{2-x}O_4$ ($0 \le x \le 0.5$) ferrite nanoparticles, Ceram. Int. 41 (2015) 8623–8629, https://doi.org/10.1016/j.ceramint.2015.03.072.
[183] S. Kumar, T.J. Shinde, P.N. Vasambekar, Study of conduction phenomena in indium substituted Mn-Zn nanoferrites, J. Magn. Magn Mater. 379 (2015) 179–185, https://doi.org/10.1016/j.jmmm.2014.12.031.
[184] S.J. Haralkar, R.H. Kadam, S.S. More, S.E. Shirsath, M.L. Mane, S. Patil, D.R. Mane, Intrinsic magnetic, structural and resistivity properties of ferromagnetic Mn 0.5 Zn 0.5 Al x Fe 2-x O 4 nanoparticles, Mater. Res. Bull. 48 (2013) 1189–1196, https://doi.org/10.1016/j.materresbull.2012.12.018.
[185] Z. Duan, J. Xu, Effects of sol concentration on the structure and magnetic properties of sol-gel MnZn ferrites, Integrated Ferroelectrics Int. J. 190 (2018) 112–119, https://doi.org/10.1080/10584587.2018.1457344.
[186] M.A. Gabal, R.S. Al-Luhaibi, Y.M. Al Angari, Mn-Zn nano-crystalline ferrites synthesized from spent Zn-C batteries using novel gelatin method, J. Hazard Mater. 246–247 (2013) 227–233, https://doi.org/10.1016/j.jhazmat.2012.12.026.
[187] K. Jalaiah, K. Vijaya Babu, Structural, magnetic and electrical properties of nickel doped Mn-Zn spinel ferrite synthesized by sol-gel method, J. Magn. Magn Mater. 423 (2017) 275–280, https://doi.org/10.1016/j.jmmm.2016.09.114.
[188] M.R. Syue, F.J. Wei, C.S. Chou, C.M. Fu, Magnetic and electrical properties of Mn-Zn ferrites synthesized by combustion method without subsequent heat treatments, J. Appl. Phys. 109 (2011) 2013–2016, https://doi.org/10.1063/1.3560880.
[189] V.J. Angadi, L. Choudhury, K. Sadhana, H.L. Liu, R. Sandhya, S. Matteppanavar, B. Rudraswamy, V. Pattar, R.V. Anavekar, K. Praveena, Structural, electrical and magnetic properties of Sc3+ doped Mn-Zn ferrite nanoparticles, J. Magn. Magn Mater. 424 (2017) 1–11, https://doi.org/10.1016/j.jmmm.2016.10.050.
[190] M.D. Rahaman, K.K. Nahar, M.N.I. Khan, A.K.M. Akther Hossain, Synthesis, structural, and electromagnetic properties of Mn0.5Zn0.5-xMgxFe2O4 (x = 0.0, 0.1) polycrystalline ferrites, Phys. B Condens. Matter 481 (2016) 156–164, https://doi.org/10.1016/j.physb.2015.11.008.
[191] G. Kogias, V. Zaspalis, New MnZn ferrite with low losses at 500 kHz over a broad temperature range, Physics Procedia, Elsevier B.V., 2015, pp. 1286–1293, , https://doi.org/10.1016/j.phpro.2015.12.143.
[192] V Tsakaloudi, G Kogias, V. T ZaspalisVasiliki Tsakaloudi1,a),, A new power MnZn ferrite for broad temperature range applications, AIP Advances 9 (2019) 035212–035214, https://doi.org/10.1063/1.5079939.
[193] M.D. Rahaman, M. Dalim Mia, M.N.I. Khan, A.K.M. Akther Hossain, Study the effect of sintering temperature on structural, microstructural and electromagnetic properties of 10% Ca-doped Mn0.6Zn0.4Fe2O4, J. Magn. Magn Mater. 404 (2016) 238–249, https://doi.org/10.1016/j.jmmm.2015.12.029.
[194] R.B. Tangsali, S.H. Keluskar, G.K. Naik, J.S. Budkuley, Effect of sintering conditions on resistivity of nanoparticle Mn-Zn ferrite prepared by nitrilotriacetate precursor method, J. Mater. Sci. 42 (2007) 878–882, https://doi.org/10.1007/s10853-006-0017-8.
[195] R.B. Tangsali, S.H. Keluskar, G.K. Naik, J.S. Budkuley, EFFECT OF SINTERING CONDITIONS ON MAGNETIC PROPERTIES OF NANOPARTICLE Mn – Zn FERRITE SYNTHESIZED WITH NITRILOTRIACETATE PRECURSOR METHOD, Int. J. Nanosci. (2004) 589–597, https://doi.org/10.1142/s0219581x04002413 03.
[196] E. Jafarnejad, S. Khanahmadzadeh, F. Ghanbary, M. Enhessari, Synthesis, characterization and optical band gap of pirochromite (MgCr2O4) nanoparticles by stearic acid sol-gel method, Current Chemistry Letters 5 (2016) 173–180, https://doi.org/10.5267/j.ccl.2016.7.001.
[197] M. Enhessari, A. Parviz, K. Ozaee, E. Karamali, Magnetic properties and heat capacity of cotio 3 nanopowders prepared by stearic acid gel method, J. Exp. Nanosci. 5 (2010) 61–68, https://doi.org/10.1080/17458080903260936.
[198] M. Ma, Y. Zhang, X. Li, D. Fu, H. Zhang, N. Gu, Synthesis and characterization of titania-coated Mn-Zn ferrite nanoparticles, Colloid. Surface. Physicochem. Eng. Aspect. 224 (2003) 207–212, https://doi.org/10.1016/S0927-7757(03)00270-X.
[199] V. Loyau, G.Y. Wang, M. Lo Bue, F. Mazaleyrat, An analysis of Mn-Zn ferrite microstructure by impedance spectroscopy, scanning transmission electron microscopy and energy dispersion spectrometry characterizations, J. Appl. Phys. 111 (2012), https://doi.org/10.1063/1.3693544.
[200] A.H. Lu, E.L. Salabas, F. Schüth, Magnetic nanoparticles: synthesis, protection, functionalization, and application, Angew. Chem. Int. Ed. 46 (2007) 1222–1244, https://doi.org/10.1002/anie.200602866.
[201] D. Kotsikau, M. Ivanovskaya, V. Pankov, Y. Fedotova, Structure and magnetic properties of manganese-zinc-ferrites prepared by spray pyrolysis method, Solid State Sci. 39 (2015) 69–73, https://doi.org/10.1016/j.solidstatesciences.2014.11.013.
[202] R. Szewczyk, Model of the magnetostrictive hysteresis loop with local maximum, Materials 12 (2018) 105, https://doi.org/10.3390/ma12010105.
[203] P. Thakur, R. Sharma, V. Sharma, P. Sharma, Structural and optical properties of Mn0.5Zn0.5Fe2O4 nano ferrites: effect of sintering temperature, Mater. Chem. Phys. 193 (2017) 285–289, https://doi.org/10.1016/j.matchemphys.2017.02.043.
[204] G.R. Mirshekari, S.S. Daee, H. Mohseni, S. Torkian, M. Ghasemi, M. Ameriannejad, M. Hoseinizade, M. Pirnia, D. Pourjafar, M. Pourmahdavi, K. Gheisari, Structure and magnetic properties of Mn-Zn ferrite synthesized by glycine-nitrate autocombustion process, Adv. Mater. Res. 409 (2011) 520–525 https://doi.org/10.4028/www.scientific.net/amr.409.520.
[205] K. Winiarska, R. Klimkiewicz, W. Tylus, A. Sobianowska-Turek, J. Winiarski, B. Szczygieł, I. Szczygieł, Study of the catalytic activity and surface properties of manganese-zinc ferrite prepared from used batteries, J. Chem. (2019) 1–14, https://doi.org/10.1155/2019/5430904 2019.
[206] M.A. Gabal, A.M. Abdel-Daiem, Y.M. Al Angari, I.M. Ismail, Influence of Al-substitution on structural, electrical and magnetic properties of Mn-Zn ferrites nanopowders prepared via the sol-gel auto-combustion method, Polyhedron 57 (2013) 105–111, https://doi.org/10.1016/j.poly.2013.04.027.
[207] R. Valenzuela, Novel applications of ferrites, Physics Research International (2012) 1–9, https://doi.org/10.1155/2012/591839 2012.
[208] Z. Wang, A. Wu, Recent Advances in Nanoporous Membranes for Water Purification, (n.d.). doi:10.3390/nano8020065.
[209] P. Kharbanda, T. Madaan, I. Sharma, S. Vashishtha, P. Kumar, A. Chauhan, S. Mittal, J.S. Bangruwa, V. Verma, Ferrites : Magnetic Materials as an Alternate Source of Green Electrical Energy, Heliyon (2019) e01151, , https://doi.org/10.1016/j.heliyon.2019.e01151.
[210] S.M. Peymani-motlagh, N. Moeinian, M. Rostami, Effect of Gd 3 þ - , Pr 3 þ - or Sm 3 þ -substituted cobalt e zinc ferrite on photodegradation of methyl orange and cytotoxicity tests, (2019), https://doi.org/10.1016/j.jre.2019.04.010.
[211] S. Bhukal, M. Dhiman, S. Bansal, K. Tripathi, RSC Advances Fundamental and Redox Catalytic Properties for the, (2016), pp. 1360–1375, https://doi.org/10.1039/c5ra22561b.
[212] O.R.R. Manimekalai, Photocatalysis of cobalt zinc ferrite nanorods under solar light, Res. Chem. Intermed. (2018) 1–11, https://doi.org/10.1007/s11164-018-3465-2.
[213] K.K. Kefeni, B.B. Mamba, T.A.M. Msagati, Application of Spinel Ferrite Nanoparticles in Water and Wastewater Treatment: A Review, Separation and Purification Technology, (2017), https://doi.org/10.1016/j.seppur.2017.07.015.
[214] G. Fan, J. Tong, F. Li, Visible-Light-Induced Photocatalyst Based on Cobalt-Doped Zinc Ferrite Nanocrystals, Industrial & Engineering Chemistry Research 51 (2012) 13639–13647, https://doi.org/10.1021/ie201933g.
[215] S. Samadi, E. Khalili, Degradation of Methyl Red under Visible Light Using N , F-TiO 2/SiO 2/rGO Nanocomposite, (2019), https://doi.org/10.1007/s11664-019-07585-w.
[216] K. Shetty, L. Renuka, H.P. Nagaswarupa, H. Nagabhushana, ScienceDirect ICNANO 2016 morphology , impedance and photocatalytic studies, Mater. Today: Proceedings 4 (2017) 11806–11815, https://doi.org/10.1016/j.matpr.2017.09.098.
[217] H. Lee, T. Shin, J. Cheon, R. Weissleder, Recent Developments in Magnetic Diagnostic Systems, Chem. Rev. 115 (2015) 10690–10724, https://doi.org/10.1021/cr500698d.
[218] N. Lee, D. Yoo, D. Ling, M.H. Cho, T. Hyeon, J. Cheon, Iron Oxide Based Nanoparticles for Multimodal Imaging and Magnetoresponsive Therapy, Chem. Rev. 115 (19) (2015) 10637–10689, https://doi.org/10.1021/acs.chemrev.5b00112.
[219] D. Ling, N. Lee, T. Hyeon, Chemical Synthesis and Assembly of Uniformly Sized Iron Oxide Nanoparticles for Medical Applications, Acc. Chem. Res. 48 (2015) 1276–1285, https://doi.org/10.1021/acs.accounts.5b00038 5th ed..
[220] M.B. Gawande, A. Goswami, T. Asefa, H. Guo, A.V. Biradar, D. Peng, R. Zboril, R.S. Varma, Core–shell Nanoparticles: Synthesis and Applications in Catalysis and Electrocatalysis, Chemical Society Reviews. Royal Society of Chemistry 44 (2015) 7540–7590.
[221] M.B. Gawande, Y. Monga, R. Zboril, R.K. Sharma, Silica-decorated magnetic nanocomposites for catalytic applications, Coord. Chem. Rev. 288 (2015) 118–143, https://doi.org/10.1016/j.ccr.2015.01.001.
[222] S.T. Aruna, A.S. Mukasyan, Combustion synthesis and nanomaterials, Curr. Opin. Solid State Mater. Sci. 12 (2008) 44–50, https://doi.org/10.1016/j.cossms.2008.12.002.
[223] A. Ali, H. Zafar, M. Zia, I. Ul Haq, A.R. Phull, J.S. Ali, A. Hussain, Synthesis, characterization, applications, and challenges of iron oxide nanoparticles, Nanotechnol. Sci. Appl. 9 (2016) 49–67, https://doi.org/10.2147/NSA.S99986.
[224] R. Sivashankar, A.B. Sathya, K. Vasantharaj, V. Sivasubramanian, Magnetic composite an environmental super adsorbent for dye sequestration – A review, Environmental Nanotechnology, Monitoring & Management 1–2 (2014) 36–39.
[225] S. Lata, S.R. Samadder, Removal of arsenic from water using nano adsorbents and challenges : a review, J. Environ. Manag. 166 (2016) 387–406, https://doi.org/10.1016/j.jenvman.2015.10.039.
[226] A. Farheen, R. Singh, FMR and magnetic studies of RF-sputtered Mn-Zn ferrite thin films, J. Supercond. Nov. Magnetism 4 (2019), https://doi.org/10.1007/s10948-019-5038-z.
[227] S. Tokatlidis, G. Kogias, V.T. Zaspalis, Low loss MnZn ferrites for applications in the frequency region of 1–3 MHz, J. Magn. Magn Mater. 465 (2018) 727–735, https://doi.org/10.1016/j.jmmm.2018.06.056.
[228] F. Fiorillo, C. Beatrice, O. Bottauscio, E. Carmi, Eddy-current losses in Mn-Zn ferrites, IEEE Trans. Magn. 50 (2014), https://doi.org/10.1109/TMAG.2013.2279878.
[229] T.P. Todorova, A. Van Den Bossche, V.C. Valchev, A procedure for the extraction of intrinsic AC conductivity and dielectric constant of N87 Mn-Zn ferrite samples based on impedance measurements and equivalent electrical circuit modeling, IEEE Trans. Power Electron. 33 (2018) 10723–10735, https://doi.org/10.1109/TPEL.2018.2802787.
[230] C.A. Stergiou, V Zaspalis, Cobalt-induced performance instabilities of Mn – Zn Ferrite Cores, IEEE Transactions on Magnetics 54 (2018) 1–8 8th ed..
[231] M.D. Lukovic, M.V. Nikolic, N.V. Blaz, L.D. Zivanov, O.S. Aleksic, L.S. Lukic, Mn-Zn ferrite round cable EMI suppressor with deep grooves and a secondary short circuit for different frequency ranges, IEEE Trans. Magn. 49 (2013) 1172–1177, https://doi.org/10.1109/TMAG.2012.2219064.
[232] D. Witkin, D. Patel, D. Sandkulla, K. Liu, Novel Tests for the As-Manufactured Strength of Mn-Zn Ferrite Inductor Cores, American Institute of Aeronautics and

Astronautics (2012) 1–14, https://doi.org/10.2514/6.2011-2114 52nd ed..
[233] J. McLean, R. Sutton, Electric field breakdown in Wireless Power Transfer systems due to ferrite dielectric polarizability, 2016 IEEE Wireless Power Transfer Conference, WPTC 2016, Institute of Electrical and Electronics Engineers Inc., 2016, , https://doi.org/10.1109/WPT.2016.7498761.
[234] S. Yuan, Y. Huang, J. Zhou, Q. Xu, C. Song, P. Thompson, Magnetic field energy harvesting under overhead power lines, IEEE Trans. Power Electron. 30 (2015) 6191–6202, https://doi.org/10.1109/TPEL.2015.2436702.
[235] A.K. Subramani, K. Kondo, M. Tada, M. Abe, M. Yoshimura, N. Matsushita, High resistive ferrite films by a solution process for electromagnetic compatible (EMC) devices, J. Magn. Magn Mater. 321 (2009) 3979–3983, https://doi.org/10.1016/j.jmmm.2009.07.036.
[236] V. Tsakaloudi, E. Papazoglou, V.T. Zaspalis, Microwave firing of MnZn-ferrites, Mater. Sci. Eng. B: Solid-State Materials for Advanced Technology 106 (2004) 289–294, https://doi.org/10.1016/j.mseb.2003.09.043.
[237] B. Jeyadevan, C.N. Chinnasamy, K. Shinoda, K. Tohji, H. Oka, Mn–Zn ferrite with higher magnetization for temperature sensitive magnetic fluid, J. Appl. Phys. 93 (2003) 8450–8452, https://doi.org/10.1063/1.1543135.
[238] P. Thakur, R. Sharma, M. Kumar, S.C. Katyal, N.S. Negi, N. Thakur, V. Sharma, P. Sharma, Super paramagnetic la doped Mn-Zn nano ferrites: dependence on dopant content and crystallite size, Mater. Res. Express 3 (2016) 1–14, https://doi.org/10.1088/2053-1591/3/7/075001.
[239] C.S.L.N. Sridhar, C.S. Lakshmi, G. Govindraj, S. Bangarraju, L. Satyanarayana, D.M. Potukuchi, Structural, morphological, magnetic and dielectric characterization of nano-phased antimony doped manganese zinc ferrites, J. Phys. Chem. Solid. 92 (2016) 70–84, https://doi.org/10.1016/j.jpcs.2016.01.006.
[240] B. Ji, C. Tian, Q. Zhang, D. Ji, J. Yang, J. Xie, J. Si, Magnetic properties of samarium and gadolinium co-doping Mn-Zn ferrites obtained by sol-gel auto-combustion method, J. Rare Earths 34 (2016) 1017–1023, https://doi.org/10.1016/S1002-0721(16)60129-1.
[241] D.H.K. Reddy, Y.S. Yun, Spinel ferrite magnetic adsorbents: alternative future materials for water purification? Coord. Chem. Rev. 315 (2016) 90–111, https://doi.org/10.1016/j.ccr.2016.01.012.
[242] B Boutra, N Guy, M. Ozacar, M. Trari, Magnetically Separable MnFe2O4/TA/ZnO Nanocomposites for Photocatalytic Degradation of Congo Red under Visible Light, Journal of Magnetism and Magnetic Materials 497 (2020) 165994.
[243] H. Waqas, A.H. Qureshi, M. Shahzad, Effect of firing temperature on the electromagnetic properties of electronic transformer cores developed by using nanosized Mn-Zn ferrite powders, Acta Metallurgica Sinica (English Letters) 28 (2015) 159–163, https://doi.org/10.1007/s40195-014-0180-x.
[244] N.V. Blaz, M.D. Lukovic, M.V. Nikolic, O.S. Aleksic, L.D. Zivanov, Heterotube Mn-Zn ferrite bundle EMI suppressor with different magnetic coupling configurations, IEEE Trans. Magn. 50 (2014), https://doi.org/10.1109/TMAG.2014.2310436.
[245] R. Ahmad, I.H. Gul, et al., Improved electrical properties of cadmium substituted cobalt ferrites nano-particles for microwave application, J. Magn. Magn Mater. (2016) 28–35, https://doi.org/10.1016/j.jmmm.2015.12.019.
[246] S. Zahi, Nickel – zinc ferrite fabricated by sol – gel route and application in high-temperature superconducting magnetic energy storage for voltage sag solving, Mater. Des. 31 (2010) 1848–1853, https://doi.org/10.1016/j.matdes.2009.11.004.
[247] M.A. Dar, K. Majid, M. Hanief, R.K. Kotnala, J. Shah, As a potential candidate for microwave device applications, JMADE 90 (2016) 443–452, https://doi.org/10.1016/j.matdes.2015.10.151.
[248] A. Poorbafrani, F. Khademi, P. Kameli, H. Salamati, Structural , Magnetic and Microwave Properties of Eu-Doped Barium Hexaferrite Powders, Journal of Superconductivity and Novel Magnetism 25 (2012) 525–531.
[249] W. Wang, C. Zang, Q. Jiao, Synthesis, structure and electromagnetic properties of Mn-Zn ferrite by sol-gel combustion technique, J. Magn. Magn Mater. 349 (2014) 116–120, https://doi.org/10.1016/j.jmmm.2013.08.057.
[250] T.L. Phan, N. Tran, D.H. Kim, N.T. Dang, D.H. Manh, Magnetic and Magnetocaloric Properties of $Zn_{1-x}Co_xFe_2O_4$ Nanoparticles, Journal of Electronics Materials 46 (2017) 4214–4226.
[251] R. Desai, V. Davariya, K. Parekh, et al., Structural and magnetic properties of size-controlled $Mn_{0.5}Zn_{0.5}Fe_2O_4$ nanoparticles and magnetic fluids, Pramana Journal of Physics 73 (2009) 765–780.
[252] K. Praveena, K. Sadhana, S. Matteppanavar, H.L. Liu, Effect of sintering temperature on the structural, dielectric and magnetic properties of Ni0.4Zn0.2Mn0.4Fe2O4 potential for radar absorbing, J. Magn. Magn Mater. 423 (2017) 343–352, https://doi.org/10.1016/j.jmmm.2016.09.129.
[253] J.T. Jang, H. Nah, J.H Lee, S.H. Moon, M.G. Kim, J. Cheon, Critical Enhancements of MRI Contrast and Hyperthermic Effects by Dopant-Controlled Magnetic Nanoparticles, Angewandte Chemie 4 (2009) 1260–1264, https://doi.org/10.1002/ange.200805149.
[254] K. Huang, Y. Yang, Y. Qin, G. Yang, D. Yin, Sintering thermodynamics of fields activated microforming and sintering technology for fabricated MnZn ferrite microparts, Journal of Microelectromechanical Systems 23 (2014) 1389–1395, https://doi.org/10.1109/JMEMS.2014.2313651.
[255] C.C. Agrafiotis, V.T. Zaspalis, Self-propagating high-temperature synthesis of MnZn-ferrites for inductor applications, J. Magn. Magn Mater. 283 (2004) 364–374, https://doi.org/10.1016/j.jmmm.2004.06.054.
[256] C.A. Stergiou, V. Zaspalis, The role of prefiring in the development of Mn-Zn spinel ferrites for inductive power transfer, Ceram. Int. 41 (2015) 4798–4804, https://doi.org/10.1016/j.ceramint.2014.12.034.
[257] J.C. Ríos-Hurtado, A.C. Martínez-Valdés, J.R. Rangel-Méndez, J.C. Ballesteros-Pacheco, E.M. Múzquiz-Ramos, Facile synthesis and characterization of Mn x Zn 1-x Fe 2 O 4/activated carbon composites for biomedical applications, Journal of Ceramic Science and Technology 7 (2016) 289–294, https://doi.org/10.4416/JCST2016-00020.
[258] K. Praveena, K. Sadhana, S. Bharadwaj, S.R. Murthy, Development of nanocrystalline Mn–Zn ferrites for forward type DC–DC converter for switching mode power supplies, Mater. Res. Innovat. 14 (2010) 56–61, https://doi.org/10.1179/143307510x12599329343727.
[259] M.R. Syue, F.J. Wei, C.S. Chou, C.M. Fu, Magnetic, dielectric, and complex impedance properties of nanocrystalline Mn-Zn ferrites prepared by novel combustion method, Thin Solid Films 519 (2011) 8303–8306, https://doi.org/10.1016/j.tsf.2011.04.003.
[260] L. Singh, H.G. Kruger, G.E. Maguire, T. Govender, R. Parboosing, The role of nanotechnology in the treatment of viral infections, Therapeutic advances in infectious disease 4 (4) (2017) 105–131.
[261] V.D. Krishna, K. Wu, A.M. Perez, J.P. Wang, Giant magnetoresistance-based biosensor for detection of influenza A virus, Front. Microbiol. 7 (2016) 400.